

1 Nitrogen restricts future sub-arctic treeline advance in an individ- 2 ual-based dynamic vegetation model

3 Adrian Gustafson^{1,2}, Paul A. Miller^{1,2}, Robert G. Björk^{4,5}, Stefan Olin¹, Benjamin Smith^{1,3}

4 ¹Department of Physical Geography and Ecosystem Science, Lund University, Sölvegatan 12, 223 62 Lund, Sweden

5 ²Center for Environmental and Climate Science, Lund University, Sölvegatan 37, 223 62, Lund, Sweden

6 ³Hawkesbury Institute for the Environment, Western Sydney University, Penrith, NSW 2751, Australia

7 ⁴Department of Earth Sciences, University of Gothenburg, P.O. Box 460, SE-40530 Gothenburg, Sweden

8 ⁵Gothenburg Global Biodiversity Centre, P.O. Box 461, SE-405 30 Gothenburg, Sweden

9 *Correspondence to: adrian.gustafson@nateko.lu.se*

10 **Abstract.** Arctic environmental change induces shifts in high latitude plant community composition and stature with
11 implications for Arctic carbon cycling and energy exchange. Two major components of change in high latitude ecosys-
12 tems are the advancement of trees into tundra and the increased abundance and size of shrubs. How future changes in
13 key climatic and environmental drivers will affect distributions of major ecosystem types is an active area of research.
14 Dynamic Vegetation Models (DVMs) offer a way to investigate multiple and interacting drivers of vegetation distribu-
15 tion and ecosystem function. We employed the LPJ-GUESS tree individual-based DVM over the Torneträsk area, a
16 subarctic landscape in northern Sweden. Using a highly resolved climate dataset to downscale CMIP5 climate data from
17 three Global Climate Models and two 21st century future scenarios (RCP2.6 and RCP8.5) we investigated future im-
18 pacts of climate change on these ecosystems. We also performed model experiments where we factorially varied drivers
19 (climate, nitrogen deposition and [CO₂]) to disentangle the effects of each on ecosystem properties and functions. Our
20 model predicted that treelines could advance by between 45 and 195 elevational meters by 2100, depending on the sce-
21 nario. Temperature was a strong driver of vegetation change, with nitrogen availability identified as an important modu-
22 lator of treeline advance. While increased CO₂ fertilisation drove productivity increases it did not result in range shifts
23 of trees. Treeline advance was realistically simulated without any temperature dependence on growth, but biomass was
24 overestimated. Our finding that nitrogen cycling could modulate treeline advance underlines the importance of repre-
25 senting plant-soil interactions in models to project future Arctic vegetation change.

26 **Keywords:** Ecosystem model, forest-tundra ecotone, treeline, sub-Arctic, climate change impacts, ecosystem stability,
27 LPJ-GUESS, biogeophysical feedbacks.

28 1. Introduction

29 In recent decades, the Arctic has been observed to become greener (Epstein et al., 2012; Bhatt et al., 2010). Causes in-
30 clude an increased growth and abundance of shrubs (Myers-Smith et al., 2011; Elmendorf et al., 2012; Forbes et al.,
31 2010), increased vegetation stature associated with a longer growing season, and poleward advance of the Arctic
32 treeline (Bjorkman et al., 2018). Shrubs protruding through the snow and treeline advance alter surface albedo and en-
33 ergy exchange with potential feedback to the climate system (Chapin et al., 2005; Sturm, 2005; Serreze and Barry,

34 2011; Zhang et al., 2013; Zhang et al., 2018). Warming and associated changes in high latitude ecosystems have impli-
35 cations for carbon cycling through increased plant productivity, species shifts (Chapin et al., 2005; Zhang et al., 2014)
36 and increased soil organic matter (SOM) decomposition with subsequent loss of carbon to the atmosphere. Studies of
37 the Arctic carbon balance have shown that the region has been a weak sink in the past (Mcguire et al., 2009; Mcguire et
38 al., 2012; Bruhwiler et al., 2021; Virkkala et al., 2021), although uncertainty is substantial, and it is difficult to deter-
39 mine accurately the strength of this sink. How climate and environmental changes will affect the relative balance be-
40 tween the carbon uptake, i.e. photosynthesis, and release processes, i.e., autotrophic and heterotrophic respiration, will
41 determine whether the Arctic will be a source or a sink of carbon in the future.

42 Forest-tundra ecotones constitute vast transition zones where abrupt changes in ecosystem functioning occur (Hofgaard
43 et al., 2012). While a generally accepted theory of what drives treeline advance is currently lacking, several alternative
44 explanations exist. Firstly, direct effects of rising temperatures have been thoroughly discussed (e.g., Rees et al., 2020;
45 Hofgaard et al., 2019; Körner, 2015; Chapin, 1983). On the global scale, treelines have been found to correlate well
46 with a 6-7°C mean growing season ground temperature (Körner and Paulsen, 2004) and could thus be expected to fol-
47 low isotherm movement as temperatures rise. A global study of alpine treeline advance in response to warming since
48 1900 shows that 52% of treelines had advanced while the other half was stationary (47%), with only occasional in-
49 stances of retreat (1%) (Harsch et al., 2009). Similar patterns have been observed on the circumarctic scale, although
50 latitudinal treelines might be expected to shift more slowly than elevational treelines due to dispersal constraints (Rees
51 et al., 2020). As trees close to the treeline often show ample storage of non-structural carbohydrates (Hoch and Körner,
52 2012) it has been suggested that a minimum temperature requirement for wood formation, rather than productivity,
53 might constrain treeline position (Körner, 2003, 2015; Körner et al., 2016).

54 Secondly, it has been hypothesised that indirect effects of warming might be as important or more so than direct effects
55 (Sullivan et al., 2015; Chapin, 1983). For example, rising air and soil temperatures might induce increased mineralisa-
56 tion and plant availability of nitrogen in the litter layer and soil (Chapin, 1983). Increased nitrogen uptake could in turn
57 enhance plant productivity and growth (Dusenge et al., 2019). Increased nitrogen uptake as a consequence of increased
58 soil temperatures or nitrogen fertilisation have been shown to increase seedling winter survival among seedlings of
59 mountain birch (*Betula pubescens ssp. tortuosa*) – the main treeline species in Scandinavia (Weih and Karlsson, 1999;
60 Karlsson and Weih, 1996).

61 Thirdly, experiments exposing plants and ecosystems to elevated CO₂ often show increased plant productivity and bio-
62 mass increase, especially in trees (Ainsworth and Long, 2005). Terrestrial biosphere models generally emulate the same
63 response (Hickler et al., 2008; Smith et al., 2014; Piao et al., 2013). Although difficult to measure in field experiments,
64 treeline position seems unresponsive to increased [CO₂] alone (Holtmeier and Broll, 2007). Whether treelines are re-
65 sponsive to increased productivity through CO₂ fertilisation might yield insights into whether treelines are limited by
66 their productivity, i.e., photosynthesis, versus the ability to utilise assimilated carbon, i.e., wood formation. However,
67 the extent to which increased [CO₂] drives long-term tree and shrub encroachment and growth remains poorly studied.

68 For treeline migration to occur, it is not only the growth and increased stature of established trees that is important, but
69 also the recruitment and survival of new individuals beyond the existing treeline (Holtmeier and Broll, 2007). Seedlings

70 of treeline species are sometimes observed above the treeline, especially in sheltered microhabitats (Hofgaard et al.,
71 2009; Sundqvist et al., 2008). However, these individuals often display stunted growth and can be decades old, although
72 age declines with elevation (Hofgaard et al., 2009). The suitability of the tundra environment for trees to establish and
73 grow taller will thus be an important factor for the rate of treeline advance (Cairns and Moen, 2004). Interspecific com-
74 petition and herbivory are known to be important modulators of range shifts of trees (Cairns and Moen, 2004; Van Bo-
75 gaert et al., 2011; Grau et al., 2012). For instance, the presence of shrubs has been shown to limit tree seedling growth
76 (Weih and Karlsson, 1999; Grau et al., 2012), likely as a consequence of competition with tree seedlings for nitrogen.
77 Comparisons of a model incorporating only bioclimatic limits to species distributions and more ecologically complex
78 models have also suggested interspecific plant competition to be important for range shifts of trees (Epstein et al., 2007;
79 Scherrer et al., 2020). Thus, as a fourth factor, shrub-tree interactions could be important when predicting range shifts
80 such as changing treeline position under future climates. Rising temperatures have been suggested as the dominant
81 driver of increased shrub growth, especially where soil moisture is not limiting (Myers-Smith et al., 2015; Myers-Smith
82 et al., 2018). Furthermore, a changed precipitation regime, especially increased winter snowfall, might promote estab-
83 lishment of trees and shrubs through the insulating effects of snow cover with subsequent increases in seedling winter
84 survival (Hallinger et al., 2010).

85 A narrow focus on a single, e.g., summer temperature, or a few driving variables may lead to overestimation of treeline
86 advance in future projections (Hofgaard et al., 2019). Dynamic vegetation models (DVMs) offer a way to investigate
87 the influence of multiple and interacting drivers on vegetation and ecosystem processes. Model predictions may be
88 compared with observations of local treelines and ecotones to validate assumptions embedded in the models, and to in-
89 terpret causality in observed dynamics and patterns. DVMs also offer a way to extrapolate observable local phenomena
90 to broader scales, such as that of circumarctic shifts in the forest-tundra ecotone and the responsible drivers. Here, we
91 examine a subarctic forest-tundra ecotone that has undergone spatial shifts over recent decades (Callaghan et al., 2013),
92 previously attributed to climate warming. Adopting an individual-based DVM incorporating a detailed description of
93 vegetation composition and stature, and nitrogen cycle dynamics, we apply the model at high spatial resolution to com-
94 pare observed and predicted recent treeline dynamics, and project future vegetation change and its implications for car-
95 bon balance and biogeophysical vegetation-atmosphere feedbacks. In addition, we conduct three model experiments to
96 separate and interpret the impact of driving factors (climate, nitrogen deposition, [CO₂]) on vegetation in a forest-tundra
97 ecotone in Sweden's sub-arctic north.

98 **2. Materials and Methods**

99 **2.1 Study site**

100 Abisko Scientific Research station (ANS; 68°21' N, 18°49' E), situated in the mountain-fringed Abisko Valley near
101 Lake Torneträsk in northern Sweden, has a long record of ecological and climate research. The climate record dates
102 back to 1913 and is still ongoing. The area is situated in a rainshadow and is thus relatively dry despite its proximity to
103 the ocean (Callaghan et al., 2013). The forests in the lower parts of the valley consist mostly of mountain birch *Betula*
104 *pubescens ssp. czerepanovii* which is also dominant at the treeline. Treeline elevation in Abisko Valley ranges between

105 600-800 m above sea level (a.s.l.) (Callaghan et al., 2013). Other tree types in lower parts of the valley are *Sorbus aucu-*
106 *paria*, and *Populus tremula*, along with small populations of *Pinus sylvestris* which are assumed to be refugia species
107 from warmer periods during the Holocene (Berglund et al., 1996). Soils consist of glaciofluvial till and sediments. An
108 extensive summary of previous studies and the environment around Lake Torneträsk can be found in Callaghan et al.
109 (2013).

110 Our study domain covers an area of approximately 85 km² and extends from Mount Nuolja in the west to the mountain
111 Nissoncorru in the east (See Fig. 2). The northern part of our study domain is bounded by Lake Torneträsk. The mean
112 annual temperature was -0.5 ± 0.9 °C for the 30-year period 1971-2000 (Fig. 1; Table 2) with January being the coldest
113 month (-10.2 ± 3.5 °C) and July the warmest (11.3 ± 1.4 °C). Mean annual precipitation was 323 ± 66 mm for the same
114 reference period. This reference period was chosen as it is the last one in the dataset by Yang et al. (2011).

115 2.2 Ecosystem model

116 We used the LPJ-GUESS DVM as the main tool for our study (Smith et al., 2001; Smith et al., 2014; Miller and Smith,
117 2012). LPJ-GUESS is one of the most ecologically detailed models of its class, suitable for regional and global-scale
118 studies of climate impacts on vegetation, employing an individual- and patch-based representation of vegetation compo-
119 sition and structure. It simulates the dynamics of plant populations and ecosystem carbon, nitrogen, and water ex-
120 changes in response to external climate forcing. Biogeophysical processes (e.g. soil hydrology and evapotranspiration)
121 and plant physiological processes (e.g. photosynthesis, respiration, carbon allocation) are interlinked and represented
122 mechanistically. Canopy fluxes of carbon dioxide and water vapour are calculated by a coupled photosynthesis and sto-
123 matal conductance scheme based on the approach of BIOME3 (Haxeltine and Prentice, 1996). Photosynthesis is a func-
124 tion of air temperature, incoming shortwave or photosynthetically active radiation, [CO₂], and water and nutrient availa-
125 bility. Autotrophic respiration has three components - maintenance, growth, and leaf respiration. Tissue maintenance
126 respiration is dependent on soil and air temperature for root and above-ground respiration, respectively, along with a
127 dependency on tissue C:N stoichiometry. All assimilated carbon that is not consumed by autotrophic respiration, less a
128 10% flux to reproductive organs, is allocated to leaves, fine roots and, for woody PFTs, sapwood, following a set of
129 prescribed allometric relationships for each PFT, resulting in biomass, height and diameter growth (Sitch et al., 2003).
130 Consequently, an individual in the model is assumed to be carbon limited when autotrophic respiration equals or ex-
131 ceeds the amount of carbon assimilated by photosynthesis. Chronically negative carbon balance at the individual level
132 eventually results in plant death.

133 The model assumes the presence of seeds in all grid cells, meaning that simulated PFTs can establish once the climate is
134 favourable, as defined by each PFT's predefined bioclimatic limits. The competition between neighbouring plant indi-
135 viduals for light, water and nutrients, affecting establishment, growth, and mortality, is modelled explicitly. Competi-
136 tion for light and nutrients is assumed to be asymmetric, i.e., individuals with taller canopies or larger root systems will
137 be advantaged in the capture of resources under scarcity. Water uptake is divided equally among individuals according
138 to the water availability and the fraction of each PFT's roots occupying each soil layer. Individuals of the same age co-
139 occurring in a local neighbourhood or patch and belonging to the same plant functional type (PFT; see below) are as-
140 sumed identical to each other. Decomposition of plant litter and cycling of soil nutrients are represented by a CEN-

141 TURV-based soil biogeochemistry module, applied at patch scale (Smith et al., 2014). Biological N fixation is repre-
142 sented by an empirical relationship between annual evapotranspiration and nitrogen fixation (Cleveland et al., 1999).
143 LPJ-GUESS does not currently incorporate PFT-specific nitrogen fixation, which for instance may be associated with
144 species that form root nodules, such as *Alnus* spp. Additional inputs of nitrogen to the system occur through nitrogen
145 deposition or fertilisation. Nitrogen is lost from the system through leaching, gaseous emissions from soils or wildfires
146 Smith et al. (2014).

147 For this study we employed LPJ-GUESS version 4.0 (Smith et al. 2014), enhanced with Arctic-specific features (Miller
148 and Smith, 2012; Wania et al., 2009). The combined model incorporates an updated set of arctic PFTs (described be-
149 low), improved soil physics and a multi-layered dynamic snow scheme, allowing for simulation of permafrost and fro-
150 zen ground. The soil scheme includes 15 equally distributed soil layers constituting a total soil depth of 1.5 meters.

151 Vegetation in the model is represented by cohorts of individuals interacting in local communities or patches and belong-
152 ing to a number of PFTs that are distinguished by growth form (tree, shrub, herbaceous), life history strategies (shade
153 tolerant or intolerant), and phenology class (evergreen/summergreen). Herbaceous PFTs are represented as a dynamic,
154 aggregate cover of ground layer vegetation in each patch. In this study 11 PFTs were implemented (See Table S2.1 in
155 supplementary material for a description of included PFTs; see Table S2.2 in supplementary material for parameter val-
156 ues associated with each PFT). Out of these, three were tree PFTs: boreal needle-leaved evergreen trees (BNE), boreal
157 shade-intolerant evergreen tree (BINE) and boreal shade-intolerant broad-leaved summergreen tree (IBS). Correspond-
158 ing tree species present in the Torneträsk region include *Picea abies* (BNE), *Pinus sylvestris* (BINE), *Betula pubescens*
159 *spp. czerepanovii*, *Populus tremula* and *Sorbus aucuparia* (IBS). Following Wolf et al. (2008), shrub PFTs with differ-
160 ent stature were implemented as follows: tall summergreen and evergreen shrubs, corresponding to *Salix spp.* (HSS)
161 and *Juniperus communis* (HSE) and low summergreen and evergreen shrubs such as *Betula nana* (LSS) and *Empetrum*
162 *nigrum* (LSE). We also included prostrate shrubs and two herbaceous PFTs.

163 Gridcell vegetation and biogeophysical properties are calculated by averaging over a number of replicate patches, each
164 nominally 0.1 ha in area and subject to the same climate forcing. No assumptions are made about how the patches are
165 distributed within a gridcell; they are a statistical sample of equally possible disturbance/demographic histories across
166 the landscape of a gridcell. Within each patch, establishment, growth and mortality of tree or shrub cohorts comprising
167 individuals of equal age (and dynamic size/form) are modelled annually (Smith et al., 2001; Smith et al., 2014). Estab-
168 lishment and mortality have both an abiotic (bioclimatic) and biotic (competition-mediated) component. Vegetation
169 dynamics, i.e. changes in the distribution and abundance of different PFTs in grid cells over time, are an emergent out-
170 come of the competition for resources between PFT cohorts at the patch level within an overall climate envelope deter-
171 mined by bioclimatic limits for establishment and survival. The bioclimatic envelope is a hard limit to vegetation distri-
172 bution, intended to represent the physiological niche of a PFT. Furthermore, the climate envelope is a proxy for physio-
173 logical processes such as meristem activity that may set species ranges, but also for climatic stressors such as tissue
174 freezing. The parameters are intended to capture broader climatic properties of each gridcell. A detailed description of
175 each bioclimatic parameter and its respective values can be found in Supplementary Table S2.2. Disturbance is ac-
176 counted for by the occasional removal of all vegetation within a patch with an annual probability of 300 yr⁻¹, represent-
177 ing random events such as storms, avalanches, insect outbreaks, and wind-throw. The study used three replicate patches

178 within each $50 \times 50\text{m}$ gridcell. We judged this number sufficient to obtain a stable representation of vegetation dynam-
179 ics given the relative area of each gridcell and replicate patches (0.1 ha). For summergreen PFTs we slightly modified
180 the assumption of a fixed growing degree day (GDD) requirement for establishment, using thawing degree days (TDD;
181 degree days with a 0°C basis; see Table S2.2) to capture the thermal sum requirement for establishment of new individ-
182 uals.

183 **2.3 Forcing data**

184 The input variables used as forcing in LPJ-GUESS simulations are monthly 2m air temperature ($^\circ\text{C}$), precipitation
185 (mm), and incoming shortwave radiation (W m^{-2}) as well as annual atmospheric $[\text{CO}_2]$ (ppm), soil texture (mineral frac-
186 tions only), and nitrogen deposition ($\text{kg N ha}^{-1} \text{ month}^{-1}$). Monthly air temperature and shortwave radiation are interpo-
187 lated to a daily time-step while precipitation is randomly distributed over the month using monthly wet-days.

188 **2.3.1 Historic period**

189 A highly resolved ($50 \times 50\text{m}$) temperature and radiation dataset using field measurements and a digital elevation model
190 (DEM) by Yang et al. (2011) provided climate input to the model simulations for the historic period (1913-2000). The
191 field measurements were conducted in the form of transects that captured mesoscale climatic variations, i.e., lapse rates.
192 In addition, the transects were placed to capture microclimatic effects of the nearby Lake Torneträsk and aspect effects
193 on radiation influx. The temperature in the lower parts of the Abisko Valley in the resulting dataset was influenced by
194 the lake with milder winters and less yearly variability. At higher elevation, the temperature was more variable over the
195 year and the local scale variations were more dependent on the different solar angles between seasons and by aspect
196 (Yang et al., 2011; Yang et al., 2012) (see Fig. S1.1; supplementary materials). For a full description of how this dataset
197 was constructed we refer to Yang et al. (2011) and Yang et al. (2012).

198 Monthly precipitation input was obtained from the Abisko Scientific Research Station weather records. Precipitation
199 was randomly distributed over each month using the number of wet-days from the CRUNCEP v.7 dataset (Wei et al.,
200 2014). We assumed that local differences in precipitation can be neglected for our study domain and thus the raw sta-
201 tion data was used as input to LPJ-GUESS for the historic period. Nitrogen deposition data for the historic and future
202 simulations were extracted from the gridcell including Abisko in the dataset of Lamarque et al. (2013). Nitrogen deposi-
203 tion was assumed to be distributed equally over the study domain.

204 Soil texture was extracted from the WISE soil dataset (Batjes, 2005) for the Abisko area and assumed to be uniform
205 across the study domain. Callaghan et al (2013) reports that the soils around the Torneträsk areas are mainly glacioflu-
206 vial till and sediments. Clay and silt fractions vary between 20-50% (Josefsson, 1990) with higher fractions of clay and
207 silt in the birch forest and a larger sand content in the heaths. In the absence of spatial information on particle size dis-
208 tributions, the soil was prescribed as a sandy loam soil with 43% sand and approximately equal fractions of silt and
209 clay.

210 **2.3.2 Future simulations**

211 Future estimates of vegetation change were simulated for one low (RCP2.6) and one high (RCP8.5) emission scenario.
212 For each scenario, climate change projections from three global climate models (GCMs) from the CMIP5 GCM ensemble
213 (Taylor et al., 2012) were used to investigate climate effects on vegetation dynamics. The chosen GCMs (MIROC-
214 ESM-CHEM, HadGEM2-AO, GFDL-ESM2M) were selected to represent the largest spread, i.e., highest, lowest and
215 near average, in modelled mean annual temperature for the reference period 2071-2100. Only models with available
216 simulations for both RCP2.6 and RCP8.5 were used in the selection. Monthly climate data for input to LPJ-GUESS
217 (temperature, total precipitation, and shortwave radiation) were extracted for the gridcell including Abisko for each
218 GCM. The number of wet-days per month was assumed not to change in the future scenario simulations, so we used the
219 1971-2000 climatology for this period.

220 The historic climate dataset by Yang et al (2011) was extended into the projection period (2001-2100) using the delta
221 change approach, as follows. For each gridcell monthly differences were calculated between the projection climate and
222 the dataset by Yang et al. (2011) for the last 30-year reference period in our historic dataset (1971-2000). For tempera-
223 ture, the arithmetic difference was extracted, while for precipitation and incoming shortwave radiation relative (i.e. geo-
224 metric) differences between the two datasets were extracted. The resulting monthly anomalies were then either added
225 (temperature) to the GCM outputs, or used to multiply (precipitation, radiation) the GCM outputs from 2001-2100, for
226 each of the climate scenarios used. Forcing data of atmospheric [CO₂] for the two scenarios were obtained from the
227 CMIP5 project.

228 **2.4 Model experiments**

229 To investigate the possible drivers of future vegetation change we performed three model experiments. The model was
230 forced with changes to one category of input (driver) variables (climate, [CO₂], nitrogen deposition) at a time for a pro-
231 jection period between the years 2001-2100. A full list of simulations can be found in Table S3 (supplementary materi-
232 als).

233 A control scenario with no climate trend (and with [CO₂] and nitrogen deposition held at their respective year 2000 val-
234 ues) was also created. We estimated the effect of the transient climate change, [CO₂] or nitrogen deposition scenarios by
235 subtracting model results for the last decade (2090-2100) in the no-trend scenario from those for the last decade (2090-
236 2100) of the respective transient scenario. To estimate how sensitive the model was to different factors, we performed a
237 Spearman rank correlation for each PFT in 50 m elevational bands over the forest-tundra ecotone. We chose Spearman
238 rank over Pearson since not all correlations were linear.

239 **2.4.1 Climate change**

240 To estimate the sensitivity to climate change the same scenarios as for the future simulations (Section 2.3.2) were used
241 while [CO₂] and nitrogen deposition were held constant at their year 2000 value.

242 Climate anomalies without any trend were created by randomly sampling full years in the last decade (1990-2000) from
243 the climate station data. The climate dataset was then extended using these data. The resulting climate scenario had the
244 same interannual variability as the historic dataset and no trend for the years 2001-2100. This scenario was used to in-
245 vestigate any lag-effects on vegetation change. This scenario also provided climate input for the nitrogen and [CO₂]
246 sensitivity tests described below.

247 **2.4.2 CO₂**

248 For our projection simulations we used five different [CO₂] scenarios from the CMIP5 project. High (RCP8.5), medium
249 (RCP6.0; RCP4.5) and low (RCP2.6) as well as a 'no change' emission scenarios were used.

250 **2.4.3 Nitrogen deposition**

251 Scenarios of nitrogen deposition were obtained from the Lamarque et al. (2013) dataset. Since this dataset assumes a
252 decrease of nitrogen deposition after year 2000 we also added four scenarios where nitrogen deposition increased with
253 2, 5, 7.5 and 10 times the nitrogen deposition relative to the year 2000. These four scenarios were created to isolate the
254 single-factor effect of nitrogen increase without any climate or [CO₂] change. The resulting additional loads of nitrogen
255 after the year 2000 in these scenarios were 0.38, 0.97, 1.46 and 1.9 gN m⁻² yr⁻¹ respectively.

256 **2.5 Model evaluation**

257 We evaluated the model against available observations in the Abisko area. Measurements of ecosystem productivity
258 from an eddy covariance (EC) tower were obtained for six non-consecutive years (Olsson et al., 2017). Biomass and
259 biomass change estimates were used to evaluate simulated biomass in the birch forest (Hedenås et al., 2011). Surveys of
260 historic vegetation change above the treeline were obtained from Rundqvist et al. (2011). Leaf area index (LAI) and
261 evapotranspiration estimates were obtained from Ovhed and Holmgren (1996).

262 The studies by Hedenås et al. (2011) and Rundqvist et al. (2011) were used to evaluate model outputs around the obser-
263 vation year 2010. To compare biomass and vegetation change with these studies we extracted five year multi-model
264 averages for 2008-2012 from our projection simulations (section 2.3.2). These means were used to calculate modelled
265 change in biomass and vegetation in our historic dataset and used to compare the modelled output to the observational
266 data.

267 To determine the local rates of treeline migration several transects were defined within our study domain (Fig. S1.2;
268 supplementary material). These transects were chosen to represent a large spread in heterogeneity with regard to slope
269 and aspect in the landscape. A subsample of the selected transects were placed close to the transects used by Van Bo-
270 gaert et al. (2011) and used to evaluate model performance. Results from the model evaluation are summarised in Table
271 1 and Table S1.1.

272 **2.6 Determination of domains in the forest-tundra ecotone**

273 In our analysis we distinguished between forest, treeline and shrub tundra, defined as follows. Any gridcell containing
274 30% fractional projective cover or more of trees was classified as forest. This limit has been used by other studies in the
275 area (e.g., Van Bogaert et al., 2011) to determine the birch forest boundary. The treeline was then determined by first
276 selecting gridcells classified as forest. Any gridcell with 4 or more neighbours fulfilling the 30% cover condition crite-
277 ria was classified as belonging to the forest. The perimeter of the forest was then determined through sorting out
278 gridcells with 4 or 5 neighbours classified as forest. Gridcells with fewer or more neighbors were regarded as tundra or
279 forest, respectively. Gridcells below the treeline were classified as forest in the analysis and gridcells above the treeline
280 were classified as tundra.

281 **2.7 Presentation of results**

282 We present seasonal values for soil and air temperature. These are averages of the three-month periods DJF, MAM,
283 JJA, and SON, referred to as winter, spring, summer and autumn below. For the RCPs average values are presented
284 with the ranges of the different scenarios within each RCP given in parenthesis. We report values of both gross primary
285 production (GPP), which we benchmark the model against, and net primary productivity (NPP) as this is of relevance
286 for the carbon limitation discussion.

287 **3. Results**

288 **3.1 Historic vegetation shifts**

289 The dominant PFT in the forest and at the treeline was IBS which constituted 90% of the total LAI (Fig. 2a-3a). The
290 only other tree PFT present in the forest was BINE, which comprised a minor fraction of total LAI. However, in the
291 lower (warmer) parts of the landscape BINE comprised up to 20% of total LAI in a few gridcells. Forest understory was
292 mixed but consisted mostly of tall and low evergreen shrubs and grasses. Shrub tundra vegetation above the treeline
293 was more mixed but LSE dominated with 51% of total LAI. Grasses comprised an additional 25% of total LAI and IBS
294 was present close to the treeline where it comprised up to 5% of LAI in some gridcells. NPP for IBS in the forest in-
295 creased from $96 \text{ gC m}^{-2} \text{ yr}^{-1}$ to $180 \text{ gC m}^{-2} \text{ yr}^{-1}$ over our historic period (1913-2000). Corresponding values at the
296 treeline did not increase but saturated at around $60 \text{ gC m}^{-2} \text{ yr}^{-1}$. Above the treeline, IBS showed very low NPP values
297 ($<15 \text{ gC m}^{-2} \text{ yr}^{-1}$), while NPP for the dominant shrub (LSE) doubled from $20 \text{ gC m}^{-2} \text{ yr}^{-1}$ at treeline to $40 \text{ gC m}^{-2} \text{ yr}^{-1}$ in
298 the tundra.

299 Between the start and end of our historic (1913-2000) simulation the treeline shifted upwards 67 elevational meters on
300 average, corresponding to a rate of 0.83 m yr^{-1} . However, during the 20th century both a period (1913-1940) with more
301 rapid warming (0.8°C) and faster tree migration rate (1.23 m yr^{-1}) as well as a period (1940-1980) with a cooling trend
302 (-0.3°C) and stationary treeline occurred (Fig. 5). Between 1913-2000, the lower boundary of the treeline shifted up-
303 wards 2 meters, while treeline upper boundaries shifted upwards 123 m. These shifts corresponded to rates of 0.03 and

304 1.54 m yr⁻¹, respectively. Similar rates were also found in the transects established to test how the model simulates het-
305 erogeneity of treeline migration (Fig. S1.2; Table S1.1; supplementary materials) where the average migration rate was
306 0.87 (0.54 - 1.25) m yr⁻¹.

307 During the 1913-2000 period, annual average air temperature at the simulated treeline warmed from -2.0°C to -0.8°C.
308 Warming occurred throughout the year but was strongest in winter and spring where temperatures increased by 3.0°C
309 and 1.4°C, respectively. In contrast, both summer and autumn temperatures warmed by only 0.6°C. The resulting win-
310 ter, spring, summer, and autumn air temperatures at the treeline in 1990-2000 were -8.7°C, 3.3°C, 8.8°C, and -0.1°C,
311 respectively. The warming was also reflected in annual average soil temperature increases of a similar magnitude, by
312 2.1°C from -0.8°C to 1.3°C. Winter soil temperature increased with 3.7°C from -5.6°C in 1913 to -1.9°C in 2000. The
313 warmer soil temperatures resulted in a 4.8% simulated increase in annual net nitrogen mineralisation rate in the treeline
314 soils over the same period. In absolute numbers, nitrogen mineralisation increased from 1.29 gN m⁻² to 1.36 gN m⁻².
315 Combined with an increased nitrogen deposition load from 0.06 gN m⁻² in 1913 to 0.20 gN m⁻² in 2000 and an increased
316 nitrogen fixation from 0.13 gN m⁻² to 0.18 gN m⁻², plant available nitrogen was simulated to increase by 15.9%. Simu-
317 lated permafrost with an active layer thickness of <1.5 m was present at elevations down to 560 m a.s.l. in a few
318 gridcells, but was always well above the treeline. More shallow permafrost (active layer thickness <1 m) was only pre-
319 sent in gridcells at elevations of 940 m a.s.l. and above.

320 **3.2 Projected vegetation shifts**

321 During the 100 year projection period (2001-2100) treelines advanced between 45 (HadGEM2-AO-RCP2.6) and 195
322 (GFDL-ESM2M-RCP8.5) elevational meters in the different scenarios, corresponding to rates of 0.45 and 1.95 eleva-
323 tional meters yr⁻¹. Total LAI increased in the entire ecotone in both RCP2.6 and RCP8.5 compared to the historic (1990-
324 2000) values (Fig. 3b-c). The increase was more pronounced in RCP8.5, which also saw a large increase in low ever-
325 green shrubs (LSE) at the end of the century (2090-2100). While the forest was still dominated by IBS, evergreen trees
326 (BNE and BINE) increased and together comprised approximately 15% of total LAI. The fraction of evergreen trees in
327 the forest correlated well with the degree of warming in each scenario. Forest GPP was mainly driven by tree PFTs and
328 increased by 50% (12% - 99%) for RCP2.6 and 177% (98% - 270%) for RCP8.5. Above the treeline, low shrubs (LSS
329 and LSE) contributed most to annual GPP change, which increased by 33% (-12% - 67%) and 239% (105% - 370%) in
330 RCP2.6 and RCP8.5, respectively. Forest NPP, wherein IBS was always dominant, increased from 200 gC m⁻² yr⁻¹ in
331 year 2000 to 300 (220-375) gC m⁻² yr⁻¹ and 490 (380-610) gC m⁻² yr⁻¹ for RCP 2.6 and RCP 8.5, respectively, over the
332 projection period. NPP for the same period for IBS at the treeline increased slightly from 60 gC m⁻² yr⁻¹ to 80 (74-90)
333 gC m⁻² yr⁻¹ and 104 (80-116) gC m⁻² yr⁻¹ for RCP2.6 and RCP8.5. Above the treeline NPP remained low (<25 gC m⁻²
334 yr⁻¹) for IBS in all scenarios and always had a lower NPP than the most productive shrub PFT (LSE). NPP for this shrub
335 was 49 (24-64) gC m⁻² yr⁻¹ and 130 (81-180) gC m⁻² yr⁻¹. The productivity increase translated into a biomass C increase
336 of the same magnitude both in the forest and above the treeline.

337 The average summer air temperature at the treeline between the last decade of the historic and projection periods in-
338 creased by 0.3°C and 6.7°C for the coldest (GFDL-ESM2M-RCP2.6) and warmest (MIROC-ESM2M-RCP8.5) GCM
339 scenario, respectively. The advance of the 6°C JJA soil temperature isotherm was more rapid than the treeline advance

340 (Fig. 4). In the two warmest scenarios (MIROC-ESM2M-RCP8.5 and HadGEM2-AO-RCP8.5) summer soil tempera-
341 tures exceeded 6°C in the whole study domain. Treeline elevations in these scenarios only reached 745 and 660 m a.s.l.,
342 respectively. Treelines advanced almost twice as fast in RCP8.5 compared to RCP2.6, 1.55 (1.10-1.96) m yr⁻¹ and 0.84
343 (0.44-1.16) m yr⁻¹, respectively.

344 3.3 Model experiments

345 A slight treeline advance at the end of the projection period (2090-2100) of approximately 11 elevational meters was
346 seen in the control simulation. As all drivers were held constant or trend-free in this simulation, this reveals a lag from
347 the historical period, likely resulting from smaller trees that had established in the historic period that matured during
348 the projection period.

349 3.3.1 Climate change

350 Treeline advance occurred in all climate change scenarios although the rate was not uniform throughout the projection
351 period (Fig. 5). When driven by climate change alone, migration rates were faster compared to simulations where nitro-
352 gen deposition and [CO₂] were also changed (Section 3.2). Treeline advance in climate change-only scenarios ranged
353 between 60 elevational meters (HadGEM2-AO-RCP2.6) and 245 elevational meters (MIROC-ESM-CHEM-RCP8.5)
354 over the 100 year projection period.

355 Tree productivity was strongly enhanced by air temperature increase over the whole study domain (Fig. 6a). Weaker
356 correlations between productivity and other climate factors such as precipitation and net shortwave radiation were also
357 seen (Fig. S1.5; S1.6; supplementary materials). Annual precipitation increased in all climate change scenarios (Table
358 2). In the lower parts of the valley, the increased precipitation did not result in increased soil moisture during summer as
359 losses through evapotranspiration driven by temperature exceeded the additional input. Spring and autumn soil moisture
360 increased in the forest, mainly because of earlier snowmelt and thawing ground in spring and relatively weaker evapo-
361 transpiration in autumn. Above the treeline, soil moisture increased as the lower temperatures and LAI did not drive
362 evapotranspiration as strongly as in the lower parts of the valley and the increased moisture input thus outweighed the
363 slightly increased evapotranspiration.

364 Increased tree productivity in the forest resulted in an increased LAI of 0.3-1.5 m² m⁻² (18-90%). BNE appeared in the
365 forest and dominated in a few gridcells. In most places BNE constituted approximately 5% of total LAI. Tall shrub
366 (HSE and HSS) productivity and LAI increased in the forest. This increase was negatively correlated with temperature,
367 i.e., increase was highest in the coolest climate change scenarios. Above the treeline, tall shrubs showed the opposite
368 pattern, increasing by 8-50% to finally constitute 10-36% of total LAI.

369 Higher soil moisture content in spring and autumn favoured trees in the whole ecotone, while forest understory suffered
370 from earlier onset of the growing season with subsequent flushing of the leaf and light shading from taller competitors.
371 Although soil moisture in summer decreased in the forest, LAI and biomass carbon of summergreen shrubs were posi-
372 tively correlated with soil moisture. A higher soil moisture during summers in the wetter GCM scenarios promoted
373 summergreen shrubs over evergreen shrubs in the whole ecotone. As an example, vegetation composition on the tundra

374 above the treeline differed between GFDL-ESM2M and MIROC-ESM-CHEM under RCP8.5, where the warmer GCM
375 showed a 52% biomass C increase in the tall evergreen shrub, HSE. The intermediate warming scenario (GFDL-
376 ESM2M-RCP8.5) showed a more mixed increase of biomass carbon in HSE (20%) and HSS (24%). While annual tem-
377 perature differed with 3.9°C between the two scenarios, average annual precipitation only differed by 6.2 mm, yielding
378 a much (26%) lower JJA soil moisture in the warmest scenario (MIROC-ESM-CHEM-RCP8.5) compared to the colder
379 (GFDL-ESM2M-RCP8.5). A relatively higher soil moisture and subsequently lower water stress allow taller plants to
380 establish.

381 Radiation correlated positively with the growth of tree PFTs, with spring and autumn radiation found to be especially
382 important for height and biomass increase (Fig. S1.7; supplementary materials). Increased radiation provided a competi-
383 tive advantage for taller trees and shrubs to shade out lower shrubs and grasses in the forest. Shrubs above the treeline
384 were also favoured by increased light.

385 Net nitrogen mineralisation at the treeline showed great variation between different climate change scenarios, ranging
386 from a 4% decrease in GFDL-ESM2M-RCP8.5 to a 79% increase in the strongest warming scenario (MIROC-ESM-
387 CHEM- RCP8.5). In absolute terms, the latter increase corresponds to an increase from 1.35 g N m⁻² yr⁻¹ at the end of
388 the historic period (1990-2000) to 2.43 g N m⁻² yr⁻¹ at the end of the century (2090-2100). This is comparable to the ni-
389 trogen load in the 7.5× increased nitrogen deposition scenario. Interestingly, despite very different plant available nitro-
390 gen and warming, the two scenarios displayed a similar resulting (2090-2100) treeline elevation (Fig. 5a).

391 Permafrost with an active layer thickness of <1.5m disappeared completely from our study domain in all scenarios ex-
392 cept the coldest (GFDL-ESM2M-RCP2.6) where it occurred in a few gridcells at elevations of approximately 600 m
393 a.s.l. However, the shallow permafrost (<1m) had disappeared also in this scenario.

394 3.3.2 CO₂

395 [CO₂] increase enhanced productivity increase in most PFTs (Fig. 6b). Total GPP averaged over the forest increased
396 between 2-10% depending on the [CO₂] scenario, with the largest increase in RCP8.5 and smallest in RCP2.6. The CO₂
397 fertilisation effect was not uniform within the landscape, but stronger towards the forest edge with increases from 2% to
398 18% from the weakest to the strongest [CO₂] scenario. NPP for IBS increased uniformly over the forest with 2.5-8.4%
399 but decreased above the treeline. Thus, the productivity of the two dominant PFTs (IBS in the forest and LSE above the
400 treeline) was reinforced in their respective domains. The increased productivity translated into a 1-5% increase in tree
401 LAI in the forest while low shrub LAI increased with 24-77%. Likewise, increase in leaf area of low shrubs was largest
402 on the tundra under elevated [CO₂], which saw a 15-40% LAI increase in the low and high [CO₂] scenario respectively.
403 Above the treeline, the productivity of grasses and low shrubs responded strongly to the CO₂ fertilisation with a 350%
404 increase in GPP for grasses and 150% increase for low shrubs. The additional litter fall produced by the increased leaf
405 mass did not lead to an increase in N mineralisation. However, immobilisation of nitrogen through increased uptake by
406 microbes increased with 2-6% between the lowest and highest [CO₂] scenarios, yielding a net reduction of plant availa-
407 ble nitrogen. Despite productivity increases, the treeline remained stationary in all [CO₂] scenarios (Fig. 5b).

408 3.3.3 Nitrogen deposition

409 Productivity of woody PFTs was in general positively correlated with nitrogen in the different nitrogen deposition sce-
410 narios. In contrast, productivity of grasses was negatively correlated (Fig. 6c) as they suffered in competition for light
411 with the trees. Annual GPP of trees (especially IBS) was positively correlated throughout the whole ecotone, but the
412 increase in GPP was larger towards the forest boundaries than in the lower parts the forest when nitrogen was added.
413 Nitrogen stressed plants in the model allocate more carbon to their roots at the expense of foliar cover when they suffer
414 a productivity reduction (Smith et al., 2014). In the two scenarios with decreasing nitrogen deposition (RCP2.6;
415 RCP8.5) there was an overall reduction in LAI in both the tundra and the forest of 6-10%. The largest reduction was
416 seen in tree PFTs, which have the largest biomass and consequently will have the highest nitrogen demand, followed by
417 tall shrubs. Low shrubs and grasses did however increase their LAI in the forest when nitrogen input decreased as a re-
418 sult of less light competition from trees. Above the treeline, LAI of low shrubs and grass PFTs also decreased with less
419 nitrogen input.

420 In all scenarios with increasing nitrogen deposition there was an advancement of the treeline in the order of 10-85 ele-
421 vational meters with smallest (2× nitrogen deposition) having the smallest change in treeline elevation and vice versa
422 for largest input (10× nitrogen deposition) (Fig. 5c). In the scenarios where nitrogen input was constant or decreasing,
423 the treeline remained stationary.

424 4. Discussion

425 In our simulations, rates of treeline advance were faster under climate change-only scenarios than when all drivers were
426 changing. This revealed nitrogen as a modulating environmental variable, as nitrogen deposition was prescribed to de-
427 crease in both the RCP2.6 and RCP8.5 scenarios. During our historic simulations, the treeline correlated well with a soil
428 temperature isotherm close to the globally observed 6-7°C isotherm. However, in our projection period the correlation
429 between the treeline position and the isotherm weakened, revealing a fading or potential lag of the treeline-climate equi-
430 librium that became stronger with increased warming. Future rates of treeline advance were thus constrained by factors
431 other than temperature in our simulations. In contrast to previous modelling studies of treeline advance (e.g., Paulsen
432 and Körner, 2014), we include not only temperature dependence on vegetation change, but also the full nitrogen cycle
433 and CO₂ fertilisation effects (Smith et al., 2014). Scenarios with increased nitrogen deposition induced treeline advance,
434 further illustrating the modulating role played by nitrogen dynamics in our results. Rising [CO₂] induced higher produc-
435 tivity in our simulations, but these productivity enhancements alone did not lead to significant treeline advance. Further-
436 more, although NPP for IBS was lower at the treeline than in the forest, it was never close to zero. Such a pattern,
437 which was seen above the treeline, indicates stagnant growth in which the carbon costs of maintaining a larger biomass
438 cancel any productivity increase. However, enhancement of productivity in combination with an allocation shift from
439 roots to shoots, enabled by a greater nitrogen uptake, favoured taller plants over their shorter neighbours in the competi-
440 tion for light within the model. For treeline advance to occur, trees need to invade the space already occupied by other
441 vegetation. As the model assumes asymmetric competition for nutrients, newly established seedlings have a disad-
442 vantage compared to incumbent vegetation, further slowing down the modelled rate of treeline advance. Field experi-
443 ments with nitrogen fertilisation have shown that mountain birch at the treeline displays enhanced growth after nitrogen

444 addition (Sveinbjörnsson et al., 1992). Furthermore, fertilisation with nitrogen improved birch seedling survival above
445 the treeline (Grau et al., 2012), and is thus likely important for establishment and growth of new individuals to form a
446 new treeline. Historically, treeline positions show a strong correlation with the 6-7°C isotherm (Körner and Paulsen,
447 2004). These records are, however, a snapshot in time and are not necessarily a strong predictor of future treeline, with
448 other factors (as for nitrogen in our results) potentially breaking the link to temperature. As pointed out by others
449 (Hofgaard et al., 2019; Van Bogaert et al., 2011), considering climate change or temperature alone in projections of
450 treeline advance could potentially result in overestimation of vegetation change. Our results clearly point to nitrogen
451 cycling as a modulating factor when predicting future Arctic vegetation shifts.

452 In our simulations, the treeline advanced at similar rates to those experienced during the historic period, resulting in a
453 displacement of 45-195 elevational meters over the 100 year projection period. Some estimates based on lake sediments
454 in the Torneträsk region from the Holocene thermal maximum, when summer temperatures may have been about 2.5°C
455 warmer than present (Kullman and Kjällgren, 2006), indicate potential treeline elevations approximately 500m above
456 present in the warmer climate (Kullman, 2010). Macrofossil records from lakes in the area indicate that birch was pre-
457 sent 300-400 meters above the current treeline (Barnekow, 1999). Furthermore, pine might have occurred approxi-
458 mately 100-150 meters above its present distribution (Berglund et al., 1996). IBS emerged as the dominant forest and
459 treeline PFT in both our historic and projection simulations, but with larger fractions of evergreen trees (BNE and
460 BINE) at the end of the century (2090-2100). Mountain birch, represented by IBS in our model, has historically domi-
461 nated treelines in the study area, even during warmer periods of the Holocene (Berglund et al., 1996), but with larger
462 populations of pine (BINE) and spruce (BNE) than seen at present. Both pine and spruce have been found in high eleva-
463 tion lake pollen sediments, and can thus be assumed to have grown in higher parts of the ecotone during warmer periods
464 (Kullman, 2010). Treeline advance for the historic period in our simulations is broadly consistent with observational
465 studies from the Abisko region (Van Bogaert et al., 2011).

466 Temperature was a strong driver of tree productivity and growth in the whole ecotone in our simulations. For the his-
467 toric period rates of treeline advance followed periods of stronger warming. However, other factors such as precipita-
468 tion indirectly influenced treeline advance through changes in vegetation composition and nitrogen mineralisation. This
469 is illustrated by the comparison of GFDL-ESM2M and MIROC-ESM-CHEM under RCP8.5, where the intermediate
470 warming but wetter scenario had very similar resulting treeline elevation as the warmer scenario. While simulated
471 treeline position was too low compared to the treeline elevation reported by Callaghan et al. (2013), the correlation with
472 the globally observed 6-7°C ground temperature isotherm (Körner and Paulsen, 2004) throughout the historic period
473 gives confidence in the model results.

474 IBS at the treeline had a positive carbon balance (NPP) and was thus not directly limited by its productivity in our simu-
475 lations. This is consistent with observations of ample carbon storage in treeline trees globally (Hoch and Körner, 2012).
476 The modelled treeline is thus not set by productivity directly but rather by competition, as non-tree PFTs become more
477 productive above the treeline. Whether the treeline is set by productivity constraints or by cold temperature limits on
478 wood formation and meristematic activity has been a subject of debate in the literature (Körner, 2015, 2003; Körner et
479 al., 2016; Fatichi et al., 2019; Pugh et al., 2016). DVMS assume NPP to be constraining for growth. On the other hand,

480 trees close to the treeline have been shown to have ample stored carbon (Hoch and Körner, 2012). Furthermore, en-
481 hancement of photosynthesis through added CO₂ does not always result in increased tree growth close to the treeline
482 (Dawes et al., 2013), and wood formation is slow below around 5°C, leading to a hypothesis of reversed control of plant
483 productivity and treeline position (Körner, 2015). As has also been highlighted in this study, ecological interactions as a
484 component in the control of treeline position has been the subject of attention in some recent modelling studies (See for
485 ex., Scherrer et al., 2020). Such studies add an extra dimension to the discussion as they do not only consider plant
486 physiology and hard limits to species distributions but also broadly accepted ecological concepts such as realised versus
487 fundamental niche.

488 The model overestimated biomass carbon in the forest but captured historic rates of biomass increase. The overestima-
489 tion was more severe closer to the forest boundaries as the model showed a weaker negative correlation between bio-
490 mass carbon and elevation than observed by Hedenås et al. (2011). The mean annual biomass increase in the same da-
491 taset is, although highly variable, on average 2.5 gC m⁻² yr⁻¹ between 1997 and 2010. As simulated GPP and LAI were
492 within the range of observations in the area (Rundqvist et al., 2011; Ovhed and Holmgren, 1996; Olsson et al., 2017),
493 this indicates a coupling between photosynthesis and growth in the model that is stronger than observed. Terrestrial bio-
494 sphere models often overestimate biomass in high latitudes (Pugh et al., 2016; Leuzinger et al., 2013) and potentially
495 lack processes that likely limit growth close to low temperature boundaries. Examples of such processes are carbon
496 costs of nitrogen acquisition (Shi et al., 2016), including costs for mycorrhizal interactions (Vowles et al., 2018), and
497 temperature limits on wood formation (Friend et al., 2019). However, data on carbon allocation and its temperature de-
498 pendence are scarce (Fatichi et al., 2019). Additionally, the overestimation in our study can be partly attributed to lack
499 of herbivory in the model. Outbreaks of the moth *Epirrita autumnata* are known to limit productivity and reduce bio-
500 mass of mountain birch in the area in certain years (Olsson et al., 2017), however, this would not fully explain the over-
501 estimation of biomass at treeline in our simulations. Since growth and biomass increment in the model do not include a
502 direct temperature dependence, nor any decoupling of growth and productivity, we do not regard these mechanisms as
503 necessary to accurately predict treeline dynamics. However, they might be important to accurately predict forest bio-
504 mass at treeline.

505 To examine variability in the simulated treeline dynamics across the study area, we established a number of transects
506 close to observation points in the landscape. Average treeline advance in the transects showed a somewhat faster and
507 more homogenous migration than reported (Van Bogaert et al., 2011). The model does not include historic anthropo-
508 genic disturbances, topographic barriers, or insect herbivory, all of which have been invoked to explain heterogeneity of
509 treeline advance rates and placement in the landscape (Van Bogaert et al., 2011; Emanuelsson, 1987). Furthermore, our
510 model does not include any wind related processes such as wind mediated snow transport or compaction. Thus, our sim-
511 ulations result in a homogenous snowpack during the winter months with no differentiation in sheltering or frost dam-
512 age that may result from different snow and ice properties. Sheltered locations in the landscape are known to promote
513 survival of tree saplings (Sundqvist et al., 2008). For nitrogen cycling this may also mean that suggested snow-shrub
514 feedbacks (Sturm et al., 2001; Sturm, 2005) are not possible to capture with the current version of our model. While
515 overall rates of treeline migration were captured, local variations arising from physical barriers such as steep slopes,
516 stony patches or anthropogenic disturbances were not possible to capture as these processes are not implemented in the
517 model. High-resolution, local observations of vertically-resolved soil texture and soil organic matter content (see, e.g.

518 Hengl et al. (2017) for an example compiled using machine-learning) have the potential to improve the spatial variability of modelled soil temperatures and nutrient cycling in our study domain.

520 A longer growing season favoured tree PFTs in the whole ecotone, which escaped early-season desiccation due to
521 milder winters and earlier spring thaw. Permafrost was only present at the highest elevations during the historic simulation but had disappeared from the landscape by 2100 for all except the coolest scenario (GFDL-ESM2M-RCP2.6). The
522 simulated permafrost was however always well above the treeline and did not have a significant impact on the treeline
523 advancement. While some aspects of ground freezing are accounted for in the model, soil vertical and horizontal movement caused by frost, and amelioration of such effects in the warmer future climate, are not. Such processes could affect
524 survival and competition among the plant functional types, especially in the seedling stage when plants are most vulnerable to mechanical disturbance (Holtmeier and Broll, 2007). These effects could be relevant to treeline dynamics at the
525 high grid resolution of our study but are not included in our model.

529 Higher summer soil moisture in the wetter climate scenarios shifted the ratio of summergreen to evergreen shrubs in
530 favour of the summergreen shrubs, in line with observations (Elmendorf et al., 2012). Conversely, drier scenarios
531 yielded an increased abundance of evergreen shrubs, similar to what has been observed in drier parts of the tundra heath
532 in the Abisko region (Scharn et al., 2021). Within RCP8.5, the warmest (MIROC-ESM-CHEM-RCP8.5) and coldest
533 (GFDL-ESM2M-RCP8.5) scenario gave rise to very similar treeline positions at the end of the projection period (2090-
534 2100). The cooler scenario led to both higher soil moisture and a greater abundance of summergreen shrubs. Higher soil
535 moisture promoted carbon allocation to the canopy, and thus favoured the taller IBS tree PFT over tall shrubs (HSS).
536 Increased shrub abundance and nutrient cycling have been shown to have potentially non-linear effects on shrub growth
537 and ecosystem carbon cycling (Buckering et al., 2009; Hicks et al., 2019), and some observations indicate that changes
538 in the ratio of summergreen to evergreen shrubs, or an increased abundance of trees, might impact soil carbon loss
539 (Parker et al., 2018; Clemmensen et al., 2021). Thus, our results indicate that any future change in soil moisture conditions could play an important role in the competitive balance between shrubs and trees and for carbon balance.

541 LPJ-GUESS assumes the presence of seeds in all gridcells and PFTs may establish when the 20-year (running) average
542 climate is within PFT-specific bioclimatic limits for establishment. This assumption may overlook potential constraints
543 on plant migration rates such as seed dispersal and reproduction. On larger spatial scales, it is likely that lags in range
544 shifts would arise from these additional constraints (Rees et al., 2020; Brown et al., 2018). Models that account for dispersal limitations generally predict slower latitudinal tree migration than models driven solely by climate (Epstein et al.,
545 2007). However, on smaller spatial scales, the same models predict competitive interactions to be more dominant in
546 determining species migration rates (Scherrer et al., 2020), and this is included in our model. In a seed transplant study
547 from the Swiss alps, seed viability could not be shown to decline towards the range limits of eight European broad-
548 leaved tree species (Kollas et al., 2012; Körner et al., 2016). Similarly, gene flow above the treeline could not be shown
549 to be limited to near-treeline trees in the Abisko region (Truong et al., 2007). Furthermore, tree saplings have been reported to be common up to 100m above the present treeline (Sundqvist et al., 2008; Hofgaard et al., 2009). As environmental conditions improve, these individuals may form the new treeline.

553 Above the treeline low evergreen shrubs (LSE) dominated the vegetation in both our historic and projection simula-
554 tions. The productivity of shrubs and grasses was greatly enhanced by CO₂ fertilisation in our [CO₂] model experiment,
555 and a large proportion of tundra productivity increases in our projection simulations could be attributed to rising [CO₂].
556 Physiological effects of elevated CO₂ on Arctic and alpine tundra productivity and growth are understudied. Free Air
557 CO₂ Enrichment (FACE) experiments are generally considered the best method for quantifying long-term ecosystem
558 effects of elevated CO₂ but are extremely costly and very few have been deployed in near-treeline locations. A majority
559 of FACE experiments have been implemented in temperate forests and grasslands, yielding limited evidence of rele-
560 vance to boreal and tundra ecosystems (Hickler et al., 2008). One FACE experiment situated in a forest-tundra ecotone
561 in the Swiss Alps showed differing responses to elevated CO₂ among shrub species where *Vaccinium myrtillus* showed
562 11% increased shoot growth while *Empetrum nigrum* was unresponsive and the response of *V. gaultherioides* depended
563 on the forest type in which it was growing (Dawes et al., 2013). Our model results indicated that shrubs are carbon lim-
564 ited and shrub productivity and growth consequently are responsive to CO₂ fertilisation.

565 **5. Conclusions**

566 In this study we examined treeline dynamics in the subarctic north of Sweden using an individual-based dynamic vege-
567 tation model at high spatial resolution. The model identified nitrogen cycling and availability as important modulating
568 factors for treeline advance in a warming future climate. Internal cycling of nitrogen in soils provides the main source
569 of this usually limiting nutrient for Arctic plants (Chapin, 1983). The model performed well regarding rates of shrub
570 increase and treeline advance but overestimated biomass carbon in the treeline forest. Treeline migration rates were re-
571 alistically simulated even though the model did not represent temperature limitations on tree growth. While a decou-
572 pling between productivity and growth in the model could potentially have improved estimates of biomass carbon, it
573 was not needed to correctly predict treeline elevation. Instead, our results point to the importance of indirect effects of
574 rising temperatures on tree range shifts, especially with regard to nutrient cycling and competition between trees and
575 shrubs. Furthermore, soil moisture strongly influenced vegetation composition within the model with implications for
576 treeline advance. Improving how models represent nutrient uptake and cycling, and incorporating empirical understand-
577 ing of processes that determine tree and shrub growth, will be key to better predictions of Arctic vegetation change and
578 carbon and nitrogen cycling. Models are a valuable aid in judging the relevance of these processes for subarctic treeline
579 ecosystems.

580 **6. Author contributions**

581 AG designed the experiments with contributions from PM and SO. AG also performed necessary model code develop-
582 ments and carried out model simulations and data analysis. RGB and BS contributed scientific advice and input
583 throughout the study and contributed to the writing. AG prepared the manuscript with contributions from all co-authors.

584 **7. Competing interests**

585 The authors declare that they have no conflict of interest.

586 **8. Acknowledgements**

587 We would like to thank Professor Christian Körner and one anonymous reviewer for their thoughtful and constructive
588 reviews which greatly improved the manuscript and widened the scope of our analysis. We acknowledge the Lund Uni-
589 versity Strategic Research Areas BECC and MERGE for their financial support. Abisko Scientific Research Station
590 generously shared the data used in preparation of the future climate projections. This research was partly funded (Paul
591 A. Miller, Robert G. Björk) by the project BioDiv-Support through the 2017-2018 Belmont Forum and BiodivERsA
592 joint call for research proposals, under the BiodivScen ERA-Net COFUND programme, and with the funding organisa-
593 tions AKA (Academy of Finland contract no 326328), ANR (ANR-18-EBI4-0007), BMBF (KFZ: 01LC1810A), FOR-
594 MAS (contract no:s 2018-02434, 2018-02436, 2018-02437, 2018-02438) and MICINN (through APCIN: PCI2018-
595 093149).

596 **References**

- 597 Ainsworth, E. A. and Long, S. P.: What have we learned from 15 years of free-air CO₂ enrichment (FACE)? A meta-
598 analytic review of the responses of photosynthesis, canopy properties and plant production to rising CO₂, *New Phytol*,
599 165, 351-371, 10.1111/j.1469-8137.2004.01224.x, 2005.
- 600 Barnekow, L.: Holocene tree-line dynamics and inferred climatic changes in the Abisko area, northern Sweden, based on
601 macrofossil and pollen records, *The Holocene*, 9, 253-265, 1999.
- 602 Batjes, N. H.: ISRIC-WISE global data set of derived soil properties on a 0.5 by 0.5 degree grid (version 3.0), ISRIC –
603 World Soil Information, Wageningen, 2005.
- 604 Berglund, B. E., Barnekow, L., Hammarlund, D., Sandgren, P., and Snowball, I. F.: Holocene forest dynamics and
605 climate changes in the Abisko area, northern Sweden - the Sonesson model of vegetation history reconsidered and
606 confirmed, *Ecological Bulletins*, 45, 15-30, 1996.
- 607 Bhatt, U. S., Walker, D. A., Raynolds, M. K., Comiso, J. C., Epstein, H. E., Jia, G., Gens, R., Pinzon, J. E., Tucker, C.
608 J., Tweedie, C. E., and Webber, P. J.: Circumpolar Arctic Tundra Vegetation Change Is Linked to Sea Ice Decline,
609 *Earth Interactions*, 14, 1-20, 10.1175/2010ei315.1, 2010.
- 610 Bjorkman, A. D., Myers-Smith, I. H., Elmendorf, S. C., Normand, S., Ruger, N., Beck, P. S. A., Blach-Overgaard, A.,
611 Blok, D., Cornelissen, J. H. C., Forbes, B. C., Georges, D., Goetz, S. J., Guay, K. C., Henry, G. H. R., HilleRisLambers,
612 J., Hollister, R. D., Karger, D. N., Kattge, J., Manning, P., Prevey, J. S., Rixen, C., Schaepman-Strub, G., Thomas, H. J.
613 D., Vellend, M., Wilmking, M., Wipf, S., Carbognani, M., Hermanutz, L., Levesque, E., Molau, U., Petraglia, A.,
614 Soudzilovskaia, N. A., Spasojevic, M. J., Tomaselli, M., Vowles, T., Alatalo, J. M., Alexander, H. D., Anadon-Rosell,
615 A., Angers-Blondin, S., Beest, M. T., Berner, L., Bjork, R. G., Buchwal, A., Buras, A., Christie, K., Cooper, E. J.,
616 Dullinger, S., Elberling, B., Eskelinen, A., Frei, E. R., Grau, O., Grogan, P., Hallinger, M., Harper, K. A., Heijmans,
617 M., Hudson, J., Hulber, K., Iturrate-Garcia, M., Iversen, C. M., Jaroszynska, F., Johnstone, J. F., Jorgensen, R. H.,

618 Kaarlejarvi, E., Klady, R., Kuleza, S., Kulonen, A., Lamarque, L. J., Lantz, T., Little, C. J., Speed, J. D. M., Michelsen,
619 A., Milbau, A., Nabe-Nielsen, J., Nielsen, S. S., Ninot, J. M., Oberbauer, S. F., Olofsson, J., Onipchenko, V. G., Rumpf,
620 S. B., Semenchuk, P., Shetti, R., Collier, L. S., Street, L. E., Suding, K. N., Tape, K. D., Trant, A., Treier, U. A.,
621 Tremblay, J. P., Tremblay, M., Venn, S., Weijers, S., Zamin, T., Boulanger-Lapointe, N., Gould, W. A., Hik, D. S.,
622 Hofgaard, A., Jonsdottir, I. S., Jorgenson, J., Klein, J., Magnusson, B., Tweedie, C., Wookey, P. A., Bahn, M., Blonder,
623 B., van Bodegom, P. M., Bond-Lamberty, B., Campetella, G., Cerabolini, B. E. L., Chapin, F. S., 3rd, Cornwell, W. K.,
624 Craine, J., Dainese, M., de Vries, F. T., Diaz, S., Enquist, B. J., Green, W., Milla, R., Niinemets, U., Onoda, Y.,
625 Ordonez, J. C., Ozinga, W. A., Penuelas, J., Poorter, H., Poschlod, P., Reich, P. B., Sandel, B., Schamp, B.,
626 Sheremetev, S., and Weiher, E.: Plant functional trait change across a warming tundra biome, *Nature*, 562, 57-62,
627 10.1038/s41586-018-0563-7, 2018.

628 Brown, C. D., Dufour-Tremblay, G., Jameson, R. G., Mamet, S. D., Trant, A. J., Walker, X. J., Boudreau, S., Harper, K.
629 A., Henry, G. H. R., Hermanutz, L., Hofgaard, A., Isaeva, L., Kershaw, G. P., and Johnstone, J. F.: Reproduction as a
630 bottleneck to treeline advance across the circumarctic forest tundra ecotone, *Ecography*, 42, 137-147,
631 10.1111/ecog.03733, 2018.

632 Bruhwiler, L., Parmentier, F.-J. W., Crill, P., Leonard, M., and Palmer, P. I.: The Arctic Carbon Cycle and Its Response
633 to Changing Climate, *Current Climate Change Reports*, 7, 14-34, 10.1007/s40641-020-00169-5, 2021.

634 Buckeridge, K. M., Zufelt, E., Chu, H., and Grogan, P.: Soil nitrogen cycling rates in low arctic shrub tundra are
635 enhanced by litter feedbacks, *Plant and Soil*, 330, 407-421, 10.1007/s11104-009-0214-8, 2009.

636 Cairns, D. and Moen, J.: Herbivory Influences Tree Lines, *Journal of Ecology*, 92, 1019-1024, 2004.

637 Callaghan, T. V., Jonasson, C., Thierfelder, T., Yang, Z., Hedenas, H., Johansson, M., Molau, U., Van Bogaert, R.,
638 Michelsen, A., Olofsson, J., Gwynn-Jones, D., Bokhorst, S., Phoenix, G., Bjerke, J. W., Tommervik, H., Christensen, T.
639 R., Hanna, E., Koller, E. K., and Sloan, V. L.: Ecosystem change and stability over multiple decades in the Swedish
640 subarctic: complex processes and multiple drivers, *Philos Trans R Soc Lond B Biol Sci*, 368, 20120488,
641 10.1098/rstb.2012.0488, 2013.

642 Chapin, F. S., 3rd, Sturm, M., Serreze, M. C., McFadden, J. P., Key, J. R., Lloyd, A. H., McGuire, A. D., Rupp, T. S.,
643 Lynch, A. H., Schimel, J. P., Beringer, J., Chapman, W. L., Epstein, H. E., Euskirchen, E. S., Hinzman, L. D., Jia, G.,
644 Ping, C. L., Tape, K. D., Thompson, C. D., Walker, D. A., and Welker, J. M.: Role of land-surface changes in arctic
645 summer warming, *Science*, 310, 657-660, 10.1126/science.1117368, 2005.

646 Chapin, F. S. I.: Direct and Indirect Effects of Temperature on Arctic Plants, *Polar Biology*, 2, 47-52, 1983.

647 Clemmensen, K. E., Durling, M. B., Michelsen, A., Hallin, S., Finlay, R. D., and Lindahl, B. D.: A tipping point in
648 carbon storage when forest expands into tundra is related to mycorrhizal recycling of nitrogen, *Ecol Lett*, 24, 1193-
649 1204, 10.1111/ele.13735, 2021.

650 Cleveland, C. C., Townsend, A. R., Schimel, D. S., Fisher, H., Howarth, R. W., Hedin, L. O., Perakis, S. S., Latty, E.
651 F., Von Fischer, J. C., Elseroad, A., and Wasson, M. F.: Global patterns of terrestrial biological nitrogen (N₂) fixation
652 in natural ecosystems, *Global Biogeochemical Cycles*, 13, 623-645, 10.1029/1999gb900014, 1999.

653 Dawes, M. A., Hagedorn, F., Handa, I. T., Streit, K., Ekblad, A., Rixen, C., Körner, C., and Hättenschwiler, S.: An
654 alpine treeline in a carbon dioxide-rich world: synthesis of a nine-year free-air carbon dioxide enrichment study,
655 *Oecologia*, 171, 623-637, 10.1007/s00442-012-2576-5, 2013.

656 Dusenge, M. E., Duarte, A. G., and Way, D. A.: Plant carbon metabolism and climate change: elevated CO₂ and
657 temperature impacts on photosynthesis, photorespiration and respiration, *New Phytol*, 221, 32-49, 10.1111/nph.15283,
658 2019.

659 Elmendorf, S. C., Henry, G. H. R., Hollister, R. D., Björk, R. G., Boulanger-Lapointe, N., Cooper, E. J., Cornelissen, J.
660 H. C., Day, T. A., Dorrepaal, E., Elumeeva, T. G., Gill, M., Gould, W. A., Harte, J., Hik, D. S., Hofgaard, A., Johnson,
661 D. R., Johnstone, J. F., Jónsdóttir, I. S., Jorgenson, J. C., Klanderud, K., Klein, J. A., Koh, S., Kudo, G., Lara, M.,
662 Lévesque, E., Magnússon, B., May, J. L., Mercado-Dí'az, J. A., Michelsen, A., Molau, U., Myers-Smith, I. H.,
663 Oberbauer, S. F., Onipchenko, V. G., Rixen, C., Martin Schmidt, N., Shaver, G. R., Spasojevic, M. J., Þórhallsdóttir, Þ.
664 E., Tolvanen, A., Troxler, T., Tweedie, C. E., Villareal, S., Wahren, C.-H., Walker, X., Webber, P. J., Welker, J. M.,
665 and Wipf, S.: Plot-scale evidence of tundra vegetation change and links to recent summer warming, *Nature Climate*
666 *Change*, 2, 453-457, 10.1038/nclimate1465, 2012.

667 Emanuelsson, U.: Human Influence on Vegetation in the Torneträsk Area during the Last Three Centuries, *Ecological*
668 *Bulletins*, 38, 95-111, 1987.

669 Epstein, H. E., Kaplan, J. O., Lischke, H., and Yu, Q.: Simulating Future Changes in Arctic and Subarctic Vegetation,
670 *Computing in Science & Engineering*, 9, 12-23, 10.1109/mcse.2007.84, 2007.

671 Epstein, H. E., Raynolds, M. K., Walker, D. A., Bhatt, U. S., Tucker, C. J., and Pinzon, J. E.: Dynamics of aboveground
672 phytomass of the circumpolar Arctic tundra during the past three decades, *Environmental Research Letters*, 7,
673 10.1088/1748-9326/7/1/015506, 2012.

674 Fatichi, S., Pappas, C., Zscheischler, J., and Leuzinger, S.: Modelling carbon sources and sinks in terrestrial vegetation,
675 *New Phytol*, 221, 652-668, 10.1111/nph.15451, 2019.

676 Forbes, B. C., Fauria, M. M., and Zetterberg, P.: Russian Arctic warming and 'greening' are closely tracked by tundra
677 shrub willows, *Global Change Biology*, 16, 1542-1554, 10.1111/j.1365-2486.2009.02047.x, 2010.

678 Friend, A. D., Eckes-Shephard, A. H., Fonti, P., Rademacher, T. T., Rathgeber, C. B. K., Richardson, A. D., and
679 Turton, R. H.: On the need to consider wood formation processes in global vegetation models and a suggested
680 approach, *Annals of Forest Science*, 76, 10.1007/s13595-019-0819-x, 2019.

681 Grau, O., Ninot, J. M., Blanco-Moreno, J. M., van Logtestijn, R. S. P., Cornelissen, J. H. C., and Callaghan, T. V.:
682 Shrub-tree interactions and environmental changes drive treeline dynamics in the Subarctic, *Oikos*, 121, 1680-1690,
683 10.1111/j.1600-0706.2011.20032.x, 2012.

684 Hallinger, M., Manthey, M., and Wilmking, M.: Establishing a missing link: warm summers and winter snow cover
685 promote shrub expansion into alpine tundra in Scandinavia, *New Phytologist*, 186, 890-899, 10.1111/j.1469-
686 8137.2010.0322, 2010.

687 Harsch, M. A., Hulme, P. E., McGlone, M. S., and Duncan, R. P.: Are treelines advancing? A global meta-analysis of
688 treeline response to climate warming, *Ecol Lett*, 12, 1040-1049, 10.1111/j.1461-0248.2009.01355.x, 2009.

689 Haxeltine, A. and Prentice, I. C.: A General Model for the Light-Use Efficiency of Primary Production, *Functional
690 Ecology*, 10, **10.2307/2390165**, 1996.

691 Hedenås, H., Olsson, H., Jonasson, C., Bergstedt, J., Dahlberg, U., and Callaghan, T. V.: Changes in Tree Growth,
692 Biomass and Vegetation Over a 13-Year Period in the Swedish Sub-Arctic, *Ambio*, 40, 672-682, 10.1007/s13280-011-
693 0173-1, 2011.

694 Hengl, T., Mendes de Jesus, J., Heuvelink, G. B., Ruiperez Gonzalez, M., Kilibarda, M., Blagotic, A., Shangguan, W.,
695 Wright, M. N., Geng, X., Bauer-Marschallinger, B., Guevara, M. A., Vargas, R., MacMillan, R. A., Batjes, N. H.,
696 Leenaars, J. G., Ribeiro, E., Wheeler, I., Mantel, S., and Kempen, B.: SoilGrids250m: Global gridded soil information
697 based on machine learning, *PLoS One*, 12, e0169748, 10.1371/journal.pone.0169748, 2017.

698 Hickler, T., Smith, B., Prentice, I. C., Mjöfors, K., Miller, P., Arneth, A., and Sykes, M. T.: CO₂ fertilization in
699 temperate FACE experiments not representative of boreal and tropical forests, *Global Change Biology*, 14, 1531-1542,
700 10.1111/j.1365-2486.2008.01598.x, 2008.

701 Hicks, L. C., Rousk, K., Rinnan, R., and Rousk, J.: Soil Microbial Responses to 28 Years of Nutrient Fertilization in a
702 Subarctic Heath, *Ecosystems*, 23, 1107-1119, 10.1007/s10021-019-00458-7, 2019.

703 Hoch, G. and Körner, C.: Global patterns of mobile carbon stores in trees at the high-elevation tree line, *Global Ecology
704 and Biogeography*, 21, 861-871, 10.1111/j.1466-8238.2011.00731.x, 2012.

705 Hofgaard, A., Dalen, L., and Hytteborn, H.: Tree recruitment above the treeline and potential for climate-driven treeline
706 change, *Journal of Vegetation Science*, 20, 1133-1144, 2009.

- 707 Hofgaard, A., Harper, K. A., and Golubeva, E.: The role of the circumarctic forest–tundra ecotone for Arctic
708 biodiversity, *Biodiversity*, 13, 174-181, 10.1080/14888386.2012.700560, 2012.
- 709 Hofgaard, A., Ols, C., Drobyshev, I., Kirchhefer, A. J., Sandberg, S., and Söderström, L.: Non-stationary Response of
710 Tree Growth to Climate Trends Along the Arctic Margin, *Ecosystems*, 22, 434-451, 10.1007/s10021-018-0279-4, 2019.
- 711 Holtmeier, F. K. and Broll, G. E.: Treeline advance - driving processes and adverse factors, *Landscape Online*, 1, 1-33,
712 10.3097/lo.200701, 2007.
- 713 Josefsson, M.: The Geocology of Subalpine Heaths in the Abisko Valley, Northern Sweden. A study of periglacial
714 conditions., Department of Physical Geography, Uppsala University, Sweden, 180 pp., 1990.
- 715 Karlsson, P. S. and Weih, M.: Relationships between Nitrogen Economy and Performance in the Mountain Birch *Betula*
716 *pubescens* ssp. *tortuosa*, *Ecological Bulletins*, 71-78, 1996.
- 717 Kollas, C., Vitasse, Y., Randin, C. F., Hoch, G., and Körner, C.: Unrestricted quality of seeds in European broad-leaved
718 tree species growing at the cold boundary of their distribution, *Ann Bot*, 109, 473-480, 10.1093/aob/mcr299, 2012.
- 719 Kullman, L.: A richer, greener and smaller alpine world: review and projection of warming-induced plant cover change
720 in the Swedish Scandes, *Ambio*, 39, 159-169, 10.1007/s13280-010-0021-8, 2010.
- 721 Kullman, L. and Kjällgren, L.: Holocene pine tree-line evolution in the Swedish Scandes: Recent tree-line rise and
722 climate change in a long-term perspective, *Boreas*, 35, 159-168, 10.1111/j.1502-3885.2006.tb01119.x, 2006.
- 723 Körner, C.: Carbon limitation in trees, *Journal of Ecology*, 91, 4-17, 2003.
- 724 Körner, C.: Paradigm shift in plant growth control, *Curr Opin Plant Biol*, 25, 107-114, 10.1016/j.pbi.2015.05.003, 2015.
- 725 Körner, C. and Paulsen, J.: A World-Wide Study of High Altitude Treeline Temperatures, *Journal of Biogeography*, 31,
726 713-732, 2004.
- 727 Körner, C., Basler, D., Hoch, G., Kollas, C., Lenz, A., Randin, C. F., Vitasse, Y., and Zimmermann, N. E.: Where, why
728 and how? Explaining the low-temperature range limits of temperate tree species, *Journal of Ecology*, 104, 1079-1088,
729 10.1111/1365-2745.12574, 2016.
- 730 Lamarque, J. F., Dentener, F., McConnell, J., Ro, C. U., Shaw, M., Vet, R., Bergmann, D., Cameron-Smith, P.,
731 Dalsoren, S., Doherty, R., Faluvegi, G., Ghan, S. J., Josse, B., Lee, Y. H., MacKenzie, I. A., Plummer, D., Shindell, D.
732 T., Skeie, R. B., Stevenson, D. S., Strode, S., Zeng, G., Curran, M., Dahl-Jensen, D., Das, S., Fritzsche, D., and Nolan,
733 M.: Multi-model mean nitrogen and sulfur deposition from the Atmospheric Chemistry and Climate Model

- 734 Intercomparison Project (ACCMIP): evaluation of historical and projected future changes, *Atmospheric Chemistry and*
735 *Physics*, 13, 7997-8018, 10.5194/acp-13-7997-2013, 2013.
- 736 Leuzinger, S., Manusch, C., Bugmann, H., and Wolf, A.: A sink-limited growth model improves biomass estimation
737 along boreal and alpine tree lines, *Global Ecology and Biogeography*, 22, 924-932, 10.1111/geb.12047, 2013.
- 738 McGuire, A. D., Anderson, L. G., Christensen, T. R., Dallimore, S., Guo, L., Hayes, D. J., Heimann, M., Lorenson, T.
739 D., Macdonald, R. W., and Roulet, N.: Sensitivity of the carbon cycle in the Arctic to climate change, *Ecological*
740 *Monographs*, 79, 523-555, 10.1890/08-2025.1, 2009.
- 741 McGuire, A. D., Christensen, T. R., Hayes, D., Heroult, A., Euskirchen, E., Kimball, J. S., Koven, C., Lafleur, P.,
742 Miller, P. A., Oechel, W., Peylin, P., Williams, M., and Yi, Y.: An assessment of the carbon balance of Arctic tundra:
743 comparisons among observations, process models, and atmospheric inversions, *Biogeosciences*, 9, 3185-3204,
744 10.5194/bg-9-3185-2012, 2012.
- 745 Miller, P. A. and Smith, B.: Modelling tundra vegetation response to recent arctic warming, *Ambio*, 41 Suppl 3, 281-
746 291, 10.1007/s13280-012-0306-1, 2012.
- 747 Myers-Smith, I. H., Hik, D. S., and Aerts, R.: Climate warming as a driver of tundra shrubline advance, *Journal of*
748 *Ecology*, 106, 547-560, 10.1111/1365-2745.12817, 2018.
- 749 Myers-Smith, I. H., Forbes, B. C., Wilmking, M., Hallinger, M., Lantz, T., Blok, D., Tape, K. D., Macias-Fauria, M.,
750 Sass-Klaassen, U., Lévesque, E., Boudreau, S., Ropars, P., Hermanutz, L., Trant, A., Collier, L. S., Weijers, S.,
751 Rozema, J., Rayback, S. A., Schmidt, N. M., Schaepman-Strub, G., Wipf, S., Rixen, C., Ménard, C. B., Venn, S.,
752 Goetz, S., Andreu-Hayles, L., Elmendorf, S., Ravolainen, V., Welker, J., Grogan, P., Epstein, H. E., and Hik, D. S.:
753 Shrub expansion in tundra ecosystems: dynamics, impacts and research priorities, *Environmental Research Letters*, 6,
754 10.1088/1748-9326/6/4/045509, 2011.
- 755 Myers-Smith, I. H., Elmendorf, S. C., Beck, P. S. A., Wilmking, M., Hallinger, M., Blok, D., Tape, K. D., Rayback, S.
756 A., Macias-Fauria, M., Forbes, B. C., Speed, J. D. M., Boulanger-Lapointe, N., Rixen, C., Lévesque, E., Schmidt, N.
757 M., Baittinger, C., Trant, A. J., Hermanutz, L., Collier, L. S., Dawes, M. A., Lantz, T. C., Weijers, S., Jørgensen, R. H.,
758 Buchwal, A., Buras, A., Naito, A. T., Ravolainen, V., Schaepman-Strub, G., Wheeler, J. A., Wipf, S., Guay, K. C., Hik,
759 D. S., and Vellend, M.: Climate sensitivity of shrub growth across the tundra biome, *Nature Climate Change*, 5, 887-
760 891, 10.1038/nclimate2697, 2015.
- 761 Olsson, P.-O., Heliasz, M., Jin, H., and Eklundh, L.: Mapping the reduction in gross primary productivity in subarctic
762 birch forests due to insect outbreaks, *Biogeosciences*, 14, 1703-1719, 10.5194/bg-14-1703-2017, 2017.
- 763 Ovhed, M. and Holmgren, B.: Modelling and measuring evapotranspiration in a mountain birch forest, *Ecological*
764 *Bulletins*, 45, 31-44, 1996.

765 Parker, T. C., Sanderman, J., Holden, R. D., Blume-Werry, G., Sjogersten, S., Large, D., Castro-Diaz, M., Street, L. E.,
766 Subke, J. A., and Wookey, P. A.: Exploring drivers of litter decomposition in a greening Arctic: results from a
767 transplant experiment across a treeline, *Ecology*, 99, 2284-2294, 10.1002/ecy.2442, 2018.

768 Paulsen, J. and Körner, C.: A climate-based model to predict potential treeline position around the globe, *Alpine*
769 *Botany*, 124, 1-12, 10.1007/s00035-014-0124-0, 2014.

770 Piao, S., Sitch, S., Ciais, P., Friedlingstein, P., Peylin, P., Wang, X., Ahlstrom, A., Anav, A., Canadell, J. G., Cong, N.,
771 Huntingford, C., Jung, M., Levis, S., Levy, P. E., Li, J., Lin, X., Lomas, M. R., Lu, M., Luo, Y., Ma, Y., Myneni, R. B.,
772 Poulter, B., Sun, Z., Wang, T., Viovy, N., Zaehle, S., and Zeng, N.: Evaluation of terrestrial carbon cycle models for
773 their response to climate variability and to CO₂ trends, *Glob Chang Biol*, 19, 2117-2132, 10.1111/gcb.12187, 2013.

774 Pugh, T. A. M., Muller, C., Arneth, A., Haverd, V., and Smith, B.: Key knowledge and data gaps in modelling the
775 influence of CO₂ concentration on the terrestrial carbon sink, *J Plant Physiol*, 203, 3-15, 10.1016/j.jplph.2016.05.001,
776 2016.

777 Rees, W. G., Hofgaard, A., Boudreau, S., Cairns, D. M., Harper, K., Mamet, S., Mathisen, I., Swirad, Z., and
778 Tutubalina, O.: Is subarctic forest advance able to keep pace with climate change?, *Glob Chang Biol*, 26, 3965-3977,
779 10.1111/gcb.15113, 2020.

780 Rundqvist, S., Hedenås, H., Sandström, A., Emanuelsson, U., Eriksson, H., Jonasson, C., and Callaghan, T. V.: Tree
781 and Shrub Expansion Over the Past 34 Years at the Tree-Line Near Abisko, Sweden, *Ambio*, 40, 683-692,
782 10.1007/s13280-011-0174-0, 2011.

783 Scharn, R., Brachmann, C. G., Patchett, A., Reese, H., Bjorkman, A., Alatalo, J., Björk, R. G., Jägerbrand, A. K.,
784 Molau, U., and Björkman, M. P.: Vegetation responses to 26 years of warming at Latnjajaure Field Station, northern
785 Sweden, *Arctic Science*, 10.1139/as-2020-0042, 2021.

786 Scherrer, D., Vitasse, Y., Guisan, A., Wohlgemuth, T., Lischke, H., and Gomez Aparicio, L.: Competition and
787 demography rather than dispersal limitation slow down upward shifts of trees' upper elevation limits in the Alps,
788 *Journal of Ecology*, 108, 2416-2430, 10.1111/1365-2745.13451, 2020.

789 Serreze, M. C. and Barry, R. G.: Processes and impacts of Arctic amplification: A research synthesis, *Global and*
790 *Planetary Change*, 77, 85-96, 10.1016/j.gloplacha.2011.03.004, 2011.

791 Shi, M., Fisher, J. B., Brzostek, E. R., and Phillips, R. P.: Carbon cost of plant nitrogen acquisition: global carbon cycle
792 impact from an improved plant nitrogen cycle in the Community Land Model, *Glob Chang Biol*, 22, 1299-1314,
793 10.1111/gcb.13131, 2016.

794 Sitch, S., Smith, B., Prentice, I. C., Arneeth, A., Bondeau, A., Cramer, W., Kaplan, J. O., Levis, S., Lucht, W., Sykes, M.
795 T., Thonicke, K., and Venevsky, S.: Evaluation of ecosystem dynamics, plant geography and terrestrial carbon cycling
796 in the LPJ dynamic global vegetation model, *Global Change Biology*, 9, 161-185, 10.1046/j.1365-2486.2003.00569.x,
797 2003.

798 Smith, B., Prentice, I. C., and Sykes, M. T.: Representation of vegetation dynamics in the modelling of terrestrial
799 ecosystems: comparing two contrasting approaches within European climate space, *Global Ecology and Biogeography*,
800 10, 621-637, 10.1046/j.1466-822X.2001.t01-1-00256.x, 2001.

801 Smith, B., Wårlind, D., Arneeth, A., Hickler, T., Leadley, P., Siltberg, J., and Zaehle, S.: Implications of incorporating N
802 cycling and N limitations on primary production in an individual-based dynamic vegetation model, *Biogeosciences*, 11,
803 2027-2054, 10.5194/bg-11-2027-2014, 2014.

804 Sturm, M.: Changing snow and shrub conditions affect albedo with global implications, *Journal of Geophysical*
805 *Research*, 110, 10.1029/2005jg000013, 2005.

806 Sturm, M., Holmgren, J., McFadden, J. P., Liston, G. E., Chapin, F. S., and Racine, C. H.: Snow–Shrub Interactions in
807 Arctic Tundra: A Hypothesis with Climatic Implications, *Journal of Climate*, 14, 336-344, 10.1175/1520-
808 0442(2001)014<0336:Ssiat>2.0.Co;2, 2001.

809 Sullivan, P., Ellison, S., McNown, R., Brownlee, A., and Sveinbjörnsson, B.: Evidence of soil nutrient availability as
810 the proximate constraint on growth of treeline trees in northwest Alaska, *Ecology*, 96, 716-727, 2015.

811 Sundqvist, M. K., Björk, R. G., and Molau, U.: Establishment of boreal forest species in alpine dwarf-shrub heath in
812 subarctic Sweden, *Plant Ecology & Diversity*, 1, 67-75, 10.1080/17550870802273395, 2008.

813 Sveinbjörnsson, B., Nordell, O., and Kauhanen, H.: Nutrient relations of mountain birch growth at and below the
814 elevational tree-line in Swedish Lapland, *Functional Ecology*, 6, 213-220, 1992.

815 Taylor, K. E., Stouffer, R. J., and Meehl, G. A.: An Overview of CMIP5 and the Experiment Design, *Bulletin of the*
816 *American Meteorological Society*, 93, 485-498, 10.1175/bams-d-11-00094.1, 2012.

817 Truong, C., Palme, A. E., and Felber, F.: Recent invasion of the mountain birch *Betula pubescens* ssp. *tortuosa* above
818 the treeline due to climate change: genetic and ecological study in northern Sweden, *J Evol Biol*, 20, 369-380,
819 10.1111/j.1420-9101.2006.01190.x, 2007.

820 Van Bogaert, R., Haneca, K., Hoogesteger, J., Jonasson, C., De Dapper, M., and Callaghan, T. V.: A century of tree line
821 changes in sub-Arctic Sweden shows local and regional variability and only a minor influence of 20th century climate
822 warming, *Journal of Biogeography*, 38, 907-921, 10.1111/j.1365-2699.2010.02453.x, 2011.

823 Virkkala, A. M., Aalto, J., Rogers, B. M., Tagesson, T., Treat, C. C., Natali, S. M., Watts, J. D., Potter, S., Lehtonen,
824 A., Mauritz, M., Schuur, E. A. G., Kochendorfer, J., Zona, D., Oechel, W., Kobayashi, H., Humphreys, E., Goeckede,
825 M., Iwata, H., Lafleur, P. M., Euskirchen, E. S., Bokhorst, S., Marushchak, M., Martikainen, P. J., Elberling, B., Voigt,
826 C., Biasi, C., Sonnentag, O., Parmentier, F. W., Ueyama, M., Celis, G., St Loius, V. L., Emmerton, C. A., Peichl, M.,
827 Chi, J., Jarveoja, J., Nilsson, M. B., Oberbauer, S. F., Torn, M. S., Park, S. J., Dolman, H., Mammarella, I., Chae, N.,
828 Poyatos, R., Lopez-Blanco, E., Rojle Christensen, T., Jung Kwon, M., Sachs, T., Holl, D., and Luoto, M.: Statistical
829 upscaling of ecosystem CO₂ fluxes across the terrestrial tundra and boreal domain: regional patterns and uncertainties,
830 *Glob Chang Biol*, 10.1111/gcb.15659, 2021.

831 Vowles, T., Lindwall, F., Ekblad, A., Bahram, M., Furneaux, B. R., Ryberg, M., and Bjork, R. G.: Complex effects of
832 mammalian grazing on extramatrical mycelial biomass in the Scandes forest-tundra ecotone, *Ecol Evol*, 8, 1019-1030,
833 10.1002/ece3.3657, 2018.

834 Wania, R., Ross, I., and Prentice, I. C.: Integrating peatlands and permafrost into a dynamic global vegetation model: 1.
835 Evaluation and sensitivity of physical land surface processes, *Global Biogeochemical Cycles*, 23, n/a-n/a,
836 10.1029/2008gb003412, 2009.

837 Wei, Y., Liu, S., Huntzinger, D. N., Michalak, A. M., Viovy, N., Post, W. M., Schwalm, C. R., Schaefer, K., Jacobson,
838 A. R., Lu, C., Tian, H., Ricciuto, D. M., Cook, R. B., Mao, J., and Shi, X.: The North American Carbon Program Multi-
839 scale Synthesis and Terrestrial Model Intercomparison Project – Part 2: Environmental driver data, *Geoscientific Model*
840 *Development*, 7, 2875-2893, 10.5194/gmd-7-2875-2014, 2014.

841 Weih, M. and Karlsson, S.: The nitrogen economy of mountain birch seedlings: implications for winter survival,
842 *Journal of Ecology*, 87, 211-219, 1999.

843 Wolf, A., Callaghan, T. V., and Larson, K.: Future changes in vegetation and ecosystem function of the Barents Region,
844 *Climatic Change*, 87, 51-73, 10.1007/s10584-007-9342-4, 2008.

845 Yang, Z., Hanna, E., and Callaghan, T. V.: Modelling surface-air-temperature variation over complex terrain around
846 abisko, swedish lapland: uncertainties of measurements and models at different scales, *Geografiska Annaler: Series A,*
847 *Physical Geography*, 93, 89-112, 10.1111/j.1468-0459.2011.00005.x, 2011.

848 Yang, Z., Hanna, E., Callaghan, T. V., and Jonasson, C.: How can meteorological observations and microclimate
849 simulations improve understanding of 1913-2010 climate change around Abisko, Swedish Lapland?, *Meteorological*
850 *Applications*, 19, 454-463, 10.1002/met.276, 2012.

851 Zhang, W., Jansson, C., Miller, P. A., Smith, B., and Samuelsson, P.: Biogeophysical feedbacks enhance the Arctic
852 terrestrial carbon sink in regional Earth system dynamics, *Biogeosciences*, 11, 5503-5519, 10.5194/bg-11-5503-2014,
853 2014.

854 Zhang, W., Miller, P. A., Jansson, C., Samuelsson, P., Mao, J., and Smith, B.: Self-Amplifying Feedbacks Accelerate
855 Greening and Warming of the Arctic, *Geophysical Research Letters*, 45, 7102-7111, 10.1029/2018gl077830, 2018.

856 Zhang, W., Miller, P. A., Smith, B., Wania, R., Koenigk, T., and Döscher, R.: Tundra shrubification and tree-line
857 advance amplify arctic climate warming: results from an individual-based dynamic vegetation model, *Environmental*
858 *Research Letters*, 8, 10.1088/1748-9326/8/3/034023, 2013.

859

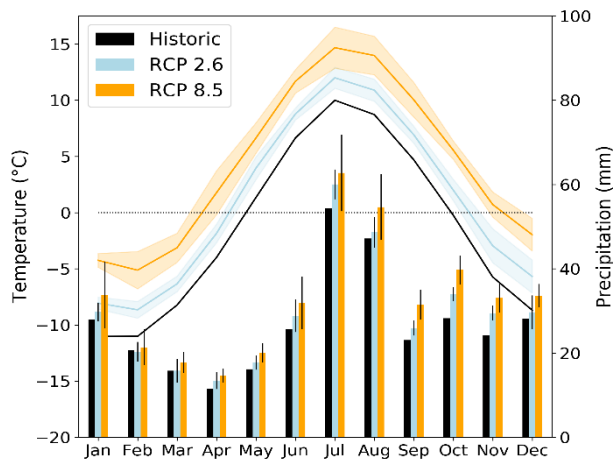


Figure 1. Historic (1971-2000) and projected (2071-2100) temperature (left) and precipitation (right) variability at the Abisko study area. The shaded areas (temperature) and black bars (precipitation) mark ± 1 standard deviation uncertainty in the three CMIP5 multi-model mean for RCP2.6 and RCP8.5 respectively.

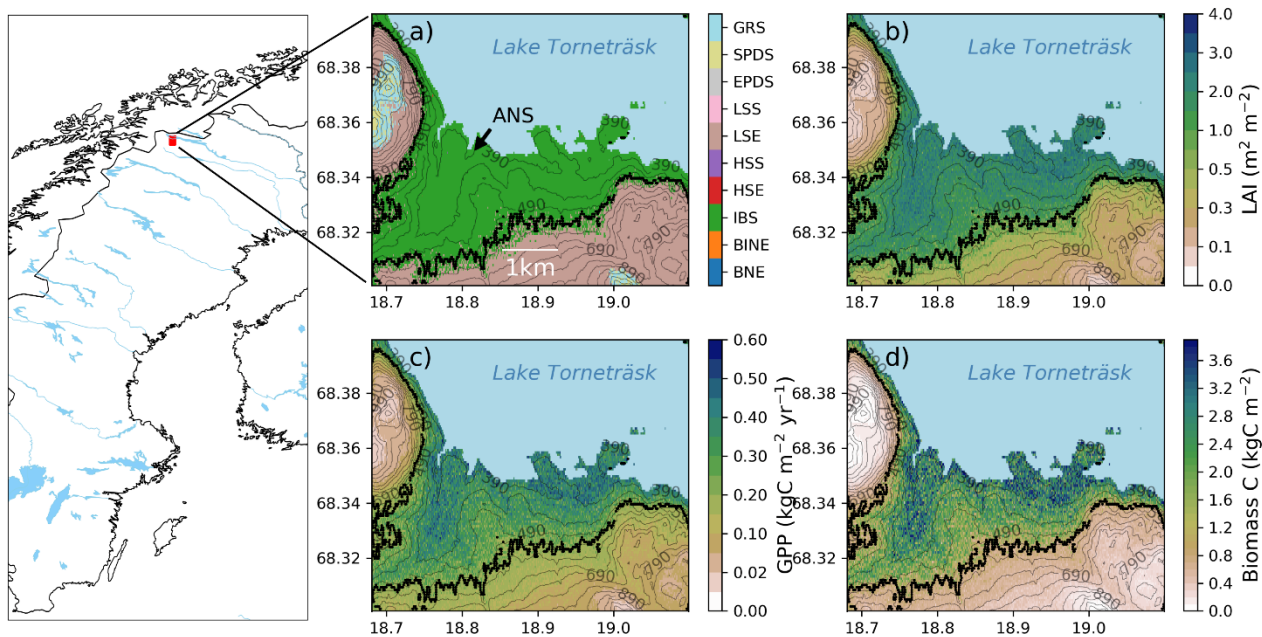


Figure 2. Map of Sweden and Scandinavia with a red square marking the study area. The location of the Abisko Scientific Research Station (ANS) is marked in panel a). Panels on the right show the study area in more detail and the modelled forest-tundra ecotone for the historic period (1990-2000). a) Dominant PFT (BNE – Boreal needle leaved evergreen tree; BINE – Boreal shade-intolerant needle leaved tree; IBS – Boreal shade-intolerant broadleaved tree; HSE – Tall evergreen shrub; HSS – Tall summergreen shrub; LSE – Low evergreen shrub; LSS – Low summergreen shrub; EPDS – Evergreen prostrate dwarf shrub; SPDS – Summergreen prostrate dwarf shrub; GRS - grasses) in the ecotone and total ecosystem b) LAI ($\text{m}^2 \text{m}^{-2}$) c) productivity (GPP; $\text{kgC m}^{-2} \text{yr}^{-1}$) and d) plant biomass carbon density (kgC m^{-2}). The black line in panels a-d shows the modelled treeline position. Numbers on the contour lines mark elevation in meters above sea level. Data source for map: Natural Earth

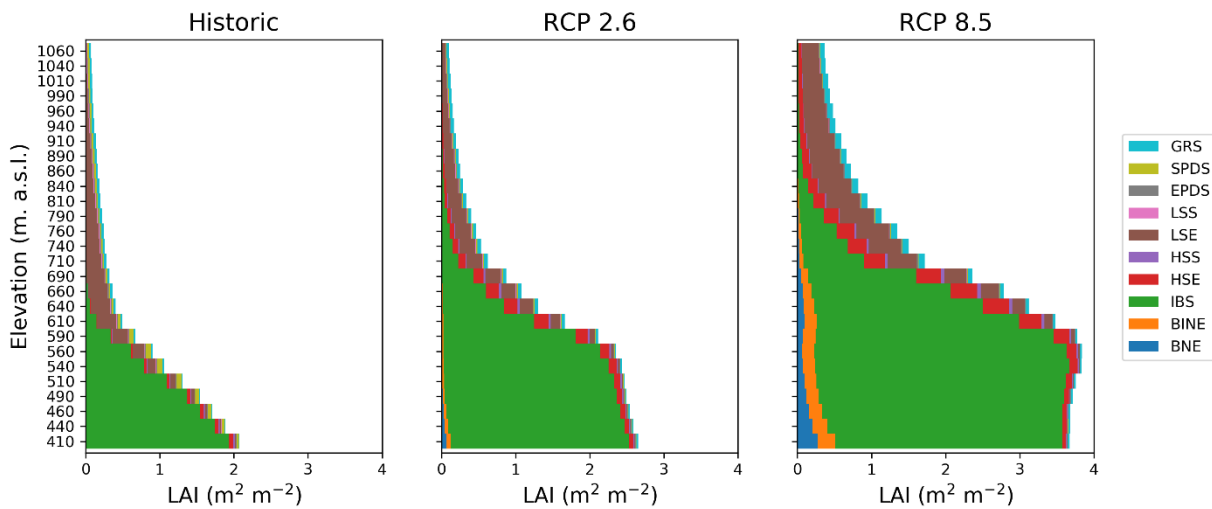


Figure 3. Leaf area index (LAI) in the forest-tundra ecotone for a) historic (1990-2000) and at the end of the century (2090-2100) for b) RCP2.6 and c) RCP8.5 respectively. Each bar represents 50 elevational meters.

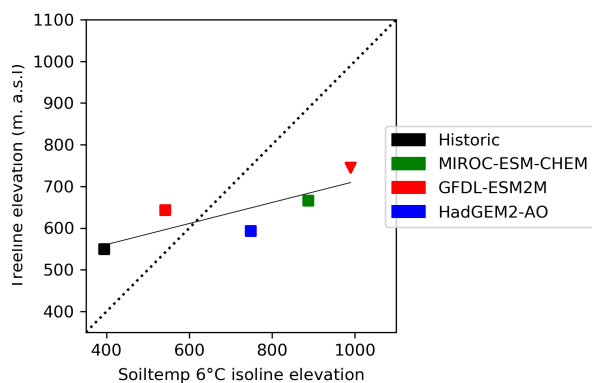


Figure 4. JJA 6°C soil temperature isotherm elevation relative to average treeline elevation. Square markers represent RCP2.6 while triangles represent RCP8.5. In the two warmest scenarios (HadGEM2-AO-RCP8.5 and MIROC-ESM-CHEM-RCP8.5), the 6°C soil temperatures exceed 6°C in the whole landscape. The dotted line represents the 1:1 relationship between treeline and isotherm placement while the solid line displays the treeline-soil temperature regression.

Table 1. Model evaluation and benchmarking results.

Parameter	Unit	Domain	Time Interval	Model value	Observed estimate	Reference
GPP (Average)	gC m ⁻² yr ⁻¹	Birch forest	2007-2014	410 ± 64	440 ± 54	Olsson et al., 2017
Carbon density	tC ha ⁻¹	Birch forest	2010	21.8 ± 10	4.39 ± 3.46	Hedenås et al., 2011
Carbon density change	%	Birch forest	1997-2010	25	19	
LAI	m ² m ⁻²	Forest canopy	1988-1989	1.65 ± 0.66	~2.0	Ovhed & Holmgren, 1996
		Understory		0.17 ± 0.12	~0.5	
Densification	%	Shrub tundra	1976-2010	+87 ± 15	+50-80	Rundqvist et al., 2011
Treeline elevation (min)	m. a.s.l.	Treeline	2010	444	~600	Callaghan et al., 2013
Treeline elevation (mean)				564	-	
Treeline elevation (max)				723	~800	
Treeline elevation change (mean)	Elevational meters	Treeline	1912-2009	80	24	van Boogart et al., 2011
Treeline elevation change (max)				123	145	
Treeline migration rate (mean)	m yr ⁻¹	Treeline	1912-2009	+0.85	+0.6	van Boogart et al., 2011
Treeline migration rate (max)				+1.18	+1.1	

Table 2. Seasonal temperature and precipitation for historic and scenario simulations.

	Season	1971-2000			2071-2100			
		Yang et al., 2011	GFDL-ESM2M		HadGEM2-AO		MIROC-ESM-CHEM	
		Historic	RCP2.6	RCP8.5	RCP2.6	RCP8.5	RCP2.6	RCP8.5
Temperature (°C)	Winter (DJF)	-9.8	-8.2	-5.4	-8.1	-4.4	-7.4	-3.1
	Spring (MAM)	-2.1	-1.3	1.0	0.4	4.11	0.7	4.8
	Summer (JJA)	9.9	10.9	13.2	11.9	14.4	13.1	13.4
	Autumn (SON)	0.1	1.1	4.2	2.3	9.1	3.2	7.2
	Annual (mean)	-0.5	0.6	3.3	1.6	5.0	2.4	6.6
Precipitation (MM)	Winter (DJF)	75	80	85	75	80	70	95
	Spring (MAM)	45	40	45	40	45	50	55
	Summer (JJA)	125	130	130	130	150	135	145
	Autumn (SON)	75	90	95	85	95	95	110
	Annual (sum)	325	340	355	335	370	350	405

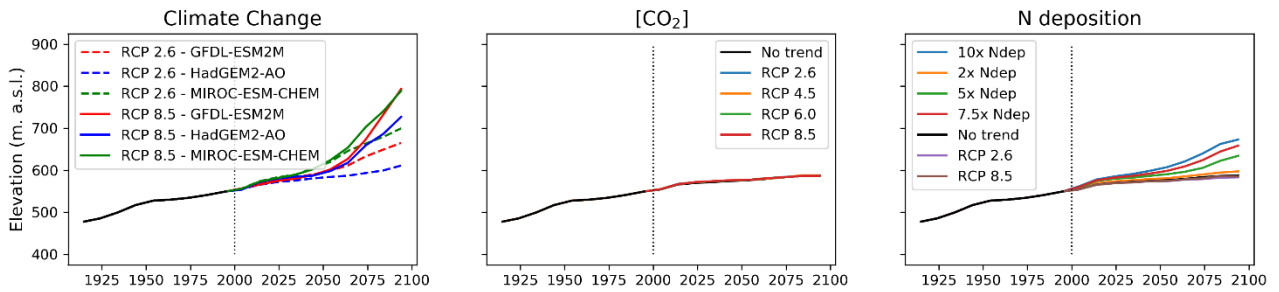


Figure 5. Shifts in average treeline elevation over the simulation period for the three experiments a) climate change b) CO₂ fertilisation and c) nitrogen deposition. Start of projection simulations are marked with a vertical dotted line in all panels. No-trend scenario in panel b-c represent a scenario where climate, CO₂ and nitrogen deposition are kept constant (without trend) relative to year 2000. Black line before year 2000 represents the historic simulation.

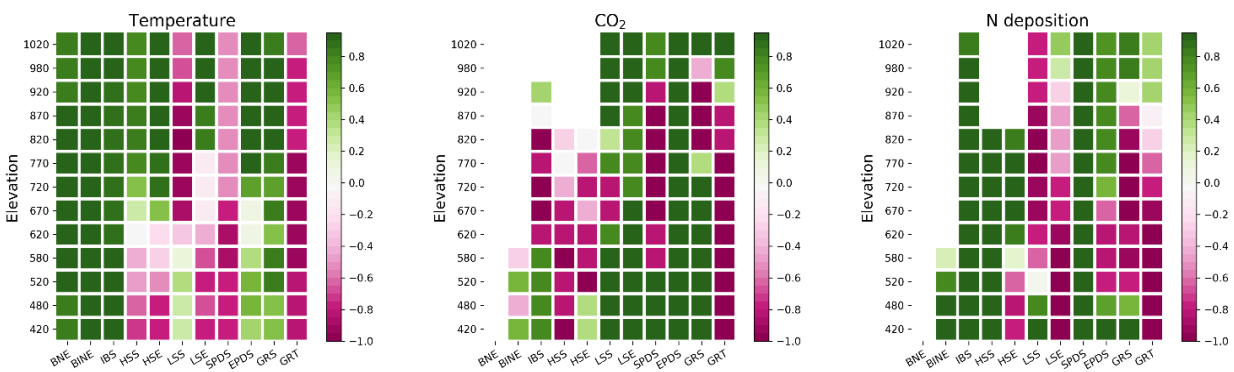


Figure 6. Correlation (Spearman rank) between annual GPP for each PFT and a) average 2090-2100 temperature anomalies in the climate change experiment, b) CO₂ scenario and c) nitrogen deposition scenario. Each box represent a 50 elevational meter band for a given PFT.